U.S. DEPARTMENT OF COMMERCE
National Technical Information Service

PB-251 548

FIELD TESTING AND EVALUATION OF METHODS FOR MEASURING VISIBILITY

NORTHWEST ENVIRONMENTAL TECHNOLOGY
LABORATORIES, INCORPORATED

PREPARED FOR
NATIONAL ENVIRONMENTAL RESEARCH CENTER

APRIL 1975

TECHNICAL REPORT DATA
(Please read Instructions on the reverse before completing)

1. REPORT NO.	2.	3. RECIPIENT'S ACCESSION NO.
EPA-650/2-75-039		

4. TITLE AND SUBTITLE	5. REPORT DATE
Field Test and Evaluation of Methods for Determining Visibility	April 1975
	6. PERFORMING ORGANIZATION CODE
7. AUTHOR(S)	8. PERFORMING ORGANIZATION REPORT NO.
Russell Cwalinski, John M. Lansinger, William G. Tank	
9. PERFORMING ORGANIZATION NAME AND ADDRESS	10. PROGRAM ELEMENT NO.
Northwest Environmental Technology Laboratories, Inc. 300-120th Avenue, N.E., Bldg. 2, Suite 108 Bellevue, Washington 98005	1A1010
	11. CONTRACT/GRANT NO.
	68-02-1209
12. SPONSORING AGENCY NAME AND ADDRESS	13. TYPE OF REPORT AND PERIOD COVERED
U.S. Environmental Sciences Research Laboratory Office of Research and Development U.S. Environmental Protection Agency Research Triangle Park, North Carolina 27711	Final Report 6-15-73/4-15/75
	14. SPONSORING AGENCY CODE

15. SUPPLEMENTARY NOTES

16. ABSTRACT

This report presents the results of a 3-month field study which was conducted to evaluate four methods for determining visibility. Three of the methods employed instruments to obtain visibility related measurements: a telephotometer measuring contrast between "black" targets and the horizon sky; a transmissometer measuring light extinction over a folded horizontal path of approximately one mile; two integrating nephelometers measuring light scattering by aerosis in a local volume of air. One nephelometer was operated at a fixed location throughout the duration of the field tests and the other on occasions at random locations. The fourth method utilized a trained observer estimating visibility in four compass directions, and this method was used as a standard for comparison. Measurements were made under a variety of meteorological conditions and results are classified by the range of relative humidity under which they were obtained.

This project has produced the result that the telephotometer measurements exhibited the highest correlation (0.88) and lowest scatter about the linear regression line relative to the local observer for all data pairs. Telephotometer measurements also exhibited the highest correlation and a nearly constant rms fractional deviation relative to the local observer with respect to relative humidity. Consequently, the results of this project identify the telephotometer as the best choice of instrument for routine estimates of daylight visibility as an indicator of air quality.

17. KEY WORDS AND DOCUMENT ANALYSIS

a. DESCRIPTORS	b. IDENTIFIERS/OPEN ENDED TERMS	c. COSATI Field/Group
*Air Pollution		13B
*Visibility		14G
*Aerosols		07D
Haze		04B
Hazemeters (meteorology)		14B
Field tests		14B
Evaluation		14G

PRICES SUBJECT TO CHANGE

18. DISTRIBUTION STATEMENT	19. SECURITY CLASS (This Report)	21. NO. OF PAGES
RELEASE TO PUBLIC	UNCLASSIFIED	98
	20. SECURITY CLASS (This page)	22. PRICE
	UNCLASSIFIED	5.00-2.25

EPA Form 2220-1 (9-73)

103002

PB 251 548

EPA-650/2-75-039

April 1975

Environmental Protection Technology Series

FIELD TESTING AND EVALUATION OF METHODS FOR MEASURING VISIBILITY

REPRODUCED BY
NATIONAL TECHNICAL
INFORMATION SERVICE
U.S. DEPARTMENT OF COMMERCE
SPRINGFIELD, VA. 22161

U.S. Environmental Protection Agency
Office of Research and Development
Washington, DC 20460

EPA-650/2-75-039

FIELD TESTING AND EVALUATION OF METHODS FOR MEASURING VISIBILITY

by

Russell Cwalinski, John M. Lansinger,
and William G. Tank

Northwest Environmental Technology Laboratories, Inc.
300-120th Avneue N. E., Building Two, Suite 108
Bellevue, Washington 98005

Contract No. 68-02-1209
ROAP No. 26AEK
Program Element No. 1A1010

EPA Project Officer: Dr. Thomas G. Dzubay

Chemistry and Physics Laboratory
National Environmental Research Center
Research Triangle Park, North Carolina 27711

Prepared for

U. S. ENVIRONMENTAL PROTECTION AGENCY
OFFICE OF RESEARCH AND DEVELOPMENT
WASHINGTON, D. C. 20460

April 1975

EPA REVIEW NOTICE

This report has been reviewed by the National Environmental Research Center - Research Triangle Park, Office of Research and Development, EPA, and approved for publication. Approval does not signify that the contents necessarily reflect the views and policies of the Environmental Protection Agency, nor does mention of trade names or commercial products constitute endorsement or recommendation for use.

RESEARCH REPORTING SERIES

Research reports of the Office of Research and Development, U.S. Environmental Protection Agency, have been grouped into series. These broad categories were established to facilitate further development and application of environmental technology. Elimination of traditional grouping was consciously planned to foster technology transfer and maximum interface in related fields. These series are:

1. ENVIRONMENTAL HEALTH EFFECTS RESEARCH
2. ENVIRONMENTAL PROTECTION TECHNOLOGY
3. ECOLOGICAL RESEARCH
4. ENVIRONMENTAL MONITORING
5. SOCIOECONOMIC ENVIRONMENTAL STUDIES
6. SCIENTIFIC AND TECHNICAL ASSESSMENT REPORTS
9. MISCELLANEOUS

This report has been assigned to the ENVIRONMENTAL PROTECTION TECHNOLOGY series. This series describes research performed to develop and demonstrate instrumentation, equipment and methodology to repair or prevent environmental degradation from point and non-point sources of pollution. This work provides the new or improved technology required for the control and treatment of pollution sources to meet environmental quality standards.

This document is available to the public for sale through the National Technical Information Service, Springfield, Virginia 22161.

Publication No. EPA-650/2-75-039

TABLE OF CONTENTS

	Page
List of Figures	iv
List of Tables	vi
Acknowledgements	vii
SECTIONS	
I Conclusions	1
II Recommendations	4
III Introduction	6
IV Theory	8
V Field Test Results	18
VI References	58
VII Appendices	59

FIGURES

No.		Page
1	Day- and nighttime visual ranges, defined according to the FAA visual range standards, versus the atmospheric extinction coefficient.	15
2	Regional location of study site.	19
3	Local scale site map showing target locations.	20
4	Nephelometer-humidity difference relationships.	29
5	Correlation coefficients and 95 percent confidence limits for the natural logarithms of the variables. (all observations, n=150).	34
6	Scattergram for observer visibility versus instrument visibility (telephotometer)	36
7	Scattergram for observer visibility versus instrument visibility (transmissometer)	37
8	Scattergram for observer visibility versus instrument visibility (nephelometer)	38
9	Scattergram for observer visibility versus instrument visibility (averaged nephelometer)	39
10	Scattergram for observer visibility versus airport visibility	40
11	Scattergram of the observer and telephotometer derived extinction coefficients	42
12	Scattergram of the transmissometer and telephotometer derived extinction coefficients	43
13	Scattergram of the nephelometer and telephotometer derived extinction coefficients	44
14	Scattergram of the averaged nephelometer and telephotometer derived extinction coefficients	45
15	Scattergram of the airport observer and telephotometer derived extinction coefficients	46
16	Composite error weighting function - transmissometer	54
17	Composite error weighting function - telephotometer	55
18	Relative error in the volume scattering coefficient	56

FIGURES

(cont.)

No.		Page
A1	Constant relative measurment errors	66
A2	Constant absolute measurement errors	67
A3	Relative error in the volume scattering coefficient	68
A4	Composite error weighting function - transmissometer	67
A5	Composite error weighting function - telephotomer	70

TABLES

No.		Page
1	Telephotometer Target Data	22
2	Correlation Coefficients for Humidity Ranges	28
3	Correlation Coefficients for Visual Ranges	32
4	Summary of Regression Analysis Parameters (Direct Variables)	41
5	Summary of Regression Analysis Parameters (Log-Log Variables)	47
6	Rms Fractional Deviations: Telephotometer versus Alternate Systems	49
7	Comparative Summary of Experimental Studies	50

ACKNOWLEDGEMENTS

The authors wish to acknowledge the following individuals:

Dr. Robert J. Charleson for his interest and helpful suggestions during the formative stages of this study;

Mr. Daniel Willott for his conscientious performance as the visual observer;

Mr. Lloyd Lowe for providing assistence in computer implementation of the statistical analysis routines.

SECTION I

CONCLUSIONS

This report presents the results of a three month field study which was conducted to evaluate four methods for determining visibility. Three of the methods employed instruments to obtain visibility related measurements: a telephotometer measuring constrast between "black" targets and the horizon sky; a transmissometer measuring light extinction over a folded horizontal path of approximately one mile; two integrating nephelometers measuring light scattering by aerosols in a local volume of air. One nephelometer was operated at a fixed location throughout the duration of the field tests and the other on occasions at random locations. The fourth method utilized a trained observer estimating visibility in four compass directions, and this method was used as a standard for comparison.

In presenting the following conclusions, it is drawn to the attention of the reader that the instruments that have been evaluated were "stock items", none of which were designed specifically for use as visibility monitors. No attempt was made to optimize the instruments for such use. In addition, all data acquired were used in the analysis, i.e., no attempt at subjective selection of data was made, and, furthermore, no correction factors of any type were applied to the measurements. The trained observer did not view the instrument readouts.

SUMMARY OF RESULTS

1) The highest correlation coefficient obtained for data pairs in the 0-65 percent relative humidity range was 0.69 between the telephotometer derived visibility and the observer visibility estimates.

2) Correlation coefficients obtained for visibility derived from the remaining two instrumental methods relative to the local observer visibility estimates for data pairs in the 0-65 percent relative humidity range were: 0.64 for the instantaneous nephelometer; 0.64 for the time-averaged nephelometer; and 0.09 for the transmissometer. The correlation coefficient between the airport observer visibility estimates and the local observer visibility estimates was 0.61 for data pairs in the corresponding relative humidity range.

3) The correlation coefficient for telephotometer derived visibility relative to the observer visibility estimates progressively increased from 0.69 to 0.95 as data pairs in the relative humidity ranges of 65-80, 80-90 and 90-100 percent were included in the correlation analysis.

4) The most similar set of correlation coefficients for all methods relative to the local observer were obtained for data pairs in the 0-80 percent relative humidity range. Only the transmissometer data exhibited a significant deviation (r=0.43) from the average value of 0.75.

5) The inclusion of data pairs for relative humidities in the range of 65 to 100 percent produced a general deterioration in correlation for all visibility methods excepting the telephotometer.

6) No significant increase in correlation between the nephelometer derived visibility and the local observer visibility estimates was realized by time-averaging (one-hour average) of the instantaneous nephelometer data.

7) The mobile nephelometer measurements agreed well with the fixed nephelometer measurements when both were operated simultaneously at the central site (correlation 0.95). Agreement did not diminish significantly for remote operation (correlation 0.90).

8) The correlations obtained for the nephelometer relative to the local observer are significantly lower than those previously reported by other investigators.

9) For all data pairs (0-100% RH), the rms deviation of the telephotometer derived visibility estimates was 5.7 km as contrasted with 6.2 km, 7.2 km and 7.6 km for the airport observers, nephelometers and transmissometer, respectively.

10) Correlation coefficients segregated as to prevailing visibility (as determined by the local observer) indicate that only the telephotometer derived visibilities were significantly correlated (r=0.83) with local observer estimates at the lower visibilities (0-8 km).

DISCUSSION

The outcome of this study is perhaps not surprising as the telephotometer method is most akin to that of the visual observer. The correlations obtained between the telephotometer measurements and observer estimates are quite high considering that optimal targets at non-optimal ranges were employed, that by necessity certain telephotometer observations were made on somewhat slanted paths, and that under good visibility conditions the observer could not make visual range estimates against the nearby valley walls. The high correlations, low rms deviations, small intercept value and constant rms fractional deviations as a function of relative humidity all support the conclusion that the telephotometer is the best choice of an instrument for daylight visibility measurements as indicators of air quality. Moreover, the results, in view of the siting of the experiment, carry the implication that the telephotometric method can be employed to obtain consistent results regardless of geographic location.

The results obtained for the nephelometer are significantly less favorable than those for the telephotometer, and also significantly less favorable than those obrained by previous investigators. Comparisons between measurement values of two nephelometers, between instantaneous and time averaged nephelometer measurements, between local and airport observer visibility estimates and between nephelometer and telephotometer derived visibility support the consistency of these results. The comparison between measurements of the remote nephelometer and fixed nephelometer establishes that local air mass inhomogeniety was not excessive. The lower correlations obtained for the nephelometer as compared with the telephotometer and as compared with correlations reported in previous studies, must reflect the siting of the experiment, utilization of all acquired data pairs in the analysis, and the fact that no attempt was made to adjust measurements to compensate for

instrumental characteristics (wavelength, bandwith, etc.) Whereas the telephotometer measurements were found to be relatively independent of relative humidity, the nephelometer measurements were not. Thus, the combination of a nearground field site on the floor of a valley and adjacent to a river appears to be an important factor and carries the implications that geographical location and local siting are important considerations in the use of an integrating nephelometer for visibility measurements.

The transmissometer results rank that instrument's use, as configured in the study, as third choice. Not unexpected in operating this instrument on a fixed 1.84 kilometer path (roundtrip) were problems related to laser beam bending and structure. Siting of the instrument's baseline on a slantpath (always less than 30 meters above the ground) crossing the Green River contributed to the beam-related problems. There was found to be a total lack of correlation ($r=0.09$) with observer estimates for the 55 data pairs in the 0-65 percent relative humidity range, conditions reflecting for the most part clear skies and strong solar insolation with the attendant pronounced scintillation effects, i.e., severe optical "noise" in the propagation medium. For the total set of 144 measurements, however, the correlation with observer visibility estimates was twice that obtained with the nephelometer ($r=0.44$ vs $r=0.22$). Implications in the results for the transmissometer are that under conditions of strong turbulence in the optical refractive index fields, scattering by turbulence far outweighs scattering by aerosol particles in the determination of narrow beam transmittance over long atmospheric paths. Furthermore, in addition to possible corrections for instrument response, considerations need to be given to beam geometry.

SECTION II

RECOMMENDATIONS

Based on the theoretical analysis and experimental results contained herein, it is recommended that the telephotometer be considered for development as the basic instrumental method for obtaining visibility estimates as an indicator of air quality. An automated telephotometer could be programmed to view "natural" dark objects located at optimal (relative to prevailing visibility) ranges, rather than optimal special targets (i.e., "totally" black), at non-optimal ranges. For a given region, a catalog of useful, natural targets at different ranges should be developed, with *a priori* instrinsic target and background brightness established for contrast measurement corrections. Such corrections will be small, but will add to the assurance of consistant visibility estimates.

An important recommendation for future investigations of any or all of the methods evaluated is that a much larger number of observations be assimilated, e.g., ten times as many or a minimum of 1500 measurements, to establish tighter confidence limits. (The telephotometer recommendation could be made on the basis of the high correlation and correspondingly smaller confidence limits, although the effect of sample size was evident).

Recommendation of the telephotometer is not intended to preclude further investigation and/or development of other instrumental systems as equivalent or alternate methods under established appropriate conditions. Therefore, it is recommended that further studies in different geographical regions for all instrumental methods be conducted.

It is also recommended that "standard" data correction factors (for each instrument) be derived and employed. The telephotometer having a response similar to that of the "typical" human eye obviously requires little in the way of wavelength and/or bandwidth correction. On the other hand, both the nephelometer and transmissometer data require such corrections (or equivalent internal instrument modifications).

It is recommended that criteria for instrument siting be established, based on this and previous experiments, such that more valid comparisons can be made. In doing so, it must be remembered that the measured visibility should relate to the "local" observer, i.e., persons within the local community, rather than to the region, for the value placed on the visual amenities of a local community could be unique.

The baseline to be used with a transmissometer is related to the range of visibility to be measured. As the theoretical analysis shows, the transmissometer is best suited to the measurement of low visibilities, and it therefore follows that a relatively long baseline is desirable. The three-quarter kilometer baseline chosen for this study would be marginal for a visibility standard of, say, five kilometers. It is recommended for future studies that a baseline no less than one kilometer be used.

As stated, the main problem encountered with the transmissometer was that of turbulence-induced beam structure and motion. This problem was amplified by use of one large (6.35 cm) and two small (2.54 cm) retroreflectors. It is recommended that for any similar transmissometer configuration a retroreflector array of perhaps 30 centimeter diameter consisting of many small retroreflectors (2.5 cm diam.) be utilized. Use of such an array would increase signal return, minimize sensitivity to beam structure and bending, and would return a beam totally collectable by an aperture of 7.5 centimeters diameter.

SECTION III

INTRODUCTION

Public awareness of atmospheric pollution is largely related to visibility, either through unpleasant coloration of the air or the reduced visual distance associated with increased pollution levels. Visual determination of air pollution levels are by nature largely subjective. Lighting conditions, optical properties of the atmosphere, sighting orientation, visual object qualities as well as a number of psychological variables, all of which vary according to locale and individual, have an effect on any human visibility estimate.

There has been an interest in developing an automated-instrument method for visibility determinations. Such an instrument method would reduce much of the subjective nature of determination, and would allow quantitative evaluations of prevailing visibility to establish the relationship between maintenance and attainment of air quality standards and the attendant visibility conditions in an urban environment. It would also allow continuous monitoring of selected areas and provide a broad data base for future work.

For instrumental estimates of visibility, the physical mechanism of primary interest is light extinction through light scatter and absorption. It has been demonstrated that a fairly close relationship exists between the light extinction coefficient and visual range (*Horvath, H.* and *K.E. Noll, 1969*). Instrument methods of interest to this study measure light transmittance from which the extinction coefficient can be derived, and light scatter from which the extinction coefficient can be approximated.

At present there are no federal air quality standards regarding visual range measurements as a base for air pollution control decisions (although California has expressed a State particulate standard in terms of visibility reducing particles).

The prospect of incorporating "visibility" measurements in expressions of state and federal standards requires study and evaluation of not only the relationships between visibility and emissions and control decisions, but also the instrumental methods available for visibility measurement.

The project described herein was designed 1) to compare the estimates of visibility derived from atmospheric measurements with a telephotometer, a transmissometer and an integrating nephelometer to those obtained by a trained observer at a single field site location, 2) to compare these results with those of related studies performed previously by other researchers, 3) to draw conclusions regarding the relative performance of the instruments, and 4) to make generalizations regarding the likely dependence of the instruments on geographical locations. The instruments were to be used "as is" for the field tests, with no attempt made to tailor them for the specific application. Wind speed and direction, temperature,

humidity and airborne particulate loadings were obtained as supporting data. Acquisition of a total of 150 sets of data was planned, and these data were subjected to analysis by relative humidity and visual range classification.

SECTION IV

THEORY

GENERAL

The impact of air pollution on the visual clarity of the atmosphere--and the universally negative response of the public to "dirty" air--is one of the most pervasive and readily noticed aspects of the air pollution problem. The impact derives predominantly from the interaction between light and the particles of the atmospheric aerosol. On a purely physical basis, the origin and course of this interaction can be stated in precise, unambiguous terms according to the elegant theory, developed by the German meteorologist Gustav Mie, of the scattering of light by small particles of arbitrary, complex refractive index (for an excellent presentation of the Mie scattering theory, see *Kerker, 1969*).

However, the question as to how far one can see through the atmosphere on a given occasion, or what one can see at a given distance, is not the subject of physics alone. Quite apart from the response *per se* of light to the optical properties of the atmosphere, the amount and distribution of light, natural and artificial, the characteristics of the objects looked at or looked for, and finally the properties of the human eye itself, all figure in the determination of the atmospheric "visual range." Thus, physiological and psychological considerations, as well as those purely physical in nature, enter into the development of the relationships between light, eye, target and atmosphere that yield visual range estimates from particulate loading data, or *vice versa*. The salient points of such a development relative to the impact of particulate air pollution on the visual clarity of the atmosphere follow.

THE EXTINCTION OF LIGHT

Fundamental to the subject of reduced visual range in a turbid atmosphere is the attenuation of light by the atmospheric aerosol. The simplest description of this attenuation is in terms of the Bouguer-Lambert Law, which predicts a simple exponential decay of light intensity with distance (*Kerker, 1969*). That is, given a collimated beam of monochromatic light of intrinsic intensity I_o, the apparent intensity, I, of the beam after traversing an atmospheric path of length R will be,

$$I = I_o e^{-\sigma R}, \qquad (1)$$

where σ is the atmospheric attenuation or extinction coefficient (units of reciprocal length), i.e., the space rate of diminution of light in its passage through the atmosphere.

Attenuation can be caused by scattering from, or absorption by, the particles of the atmospheric aerosol, alone or in any combination. The extinction coefficient can thus be written in terms of separate scattering and absorption coefficients, k_s and k_a, respectively, as,

$$\sigma = k_s + k_a. \tag{2}$$

The ratio of the received to the intrinsic source intensity is termed the transmittance, τ;

$$\tau \equiv \frac{I}{I_o} = e^{-\sigma R} \tag{3}$$

The Bouguer-Lambert law is valid for single scattering.

VISUAL RANGE ESTIMATES

Reduced to the simplest terms, an object is recognized when it exhibits a contrast in brightness or in color with its surroundings. During daytime, the contrast is usually in relation to dark objects against bright backgrounds; at night it is usually the opposite case, viz., bright objects (light sources) against dark backgrounds. Consider first the daytime conditions.

THE REDUCTION OF DAYLIGHT CONTRAST

In viewing remote objects through the daylight atmosphere, contrasts in both brightness and chromaticity are reduced due to light from the sun and sky that is scattered into the eyes of the observer by the particles of the atmospheric aerosol (including molecules of the atmospheric gases) in the air between him and the object. The addition of this "air-light" to the observer's field-of-view, moreover, causes an object of any color to appear nearly achromatic by the time its contrast with, say, the horizon sky has fallen to such a low value that it "blends" with the background and can no longer be recognized (*Middleton, 1952*). As a result, contrasts in brightness are much more important than contrasts in chromaticity in determining how far an object can be seen in a turbid atmosphere. It is in regard to brightness contrast alone, then, and how the atmosphere alters this contrast, that the description of daylight visibility as related to atmospheric turbidity develops.

Consider an isolated object of brightness B surrounded by a uniform and fairly extensive background of brightness B'. The brightness contrast between the object and its background is defined as,

$$C \equiv \frac{B-B'}{B'}. \tag{4}$$

Note that, in theory at least, the range of C is from -1 to $+\infty$, the former value obtaining with a perfectly "black" object (B = 0), the latter from a perfectly "black" background (B' = 0). Very large positive contrasts (but not in practice infinite) arise with the consideration of lights at night; daytime contrasts greater than 10 seldom occur (*Middleton, 1952*).

Denote, now, the brightnesses of the object and its background when seen close at hand by B_o and B'_o, and by B_R and B'_R when seen from a distance R. Then,

$$C_o = \frac{B_o - B'_o}{B'_o} \tag{5}$$

may be called the *intrinsic contrast, and*

$$C_R = \frac{B_R - B'_R}{B'_R} \tag{6}$$

the *apparent contrast.* The relationship between C_o and C_R is termed the law of contrast reduction, which, in the most general form as developed by Duntley (*1948*), takes the form

$$C_R = C_o \left[\frac{B'_o}{B'_R}\right] e^{-\sigma R} \tag{7}$$

The simplest form of equation (7) is obtained when an object is viewed horizontally against the horizon sky. In this case the background brightness is the air-light itself through the entire atmospheric depth, and it therefore will not change as the object is approached--there always remains, in effect, an "infinity" of air behind the object. For this case then, $B'_o = B'_R$, and equation (4) reduces to,

$$C_R = C_o e^{-\sigma R} \tag{8}$$

Note that in this case contrast decays with distance exactly as does transmittance [equation (3)].

DAYLIGHT VISUAL RANGE

Equation (8) describes how the contrast between an object and the adjacent horizon sky is reduced by the intervening atmosphere. If, then, a value can be assigned to the minimum, or *liminal* contrast which can be

detected by the human eye, equation (8) can be used to determine the range at which a given object can just be seen. That is, let ε represent the liminal contrast. The solution of equation (8) for R with ε substituted for C_R will then yield the range at which the apparent contrast of the object of intrinsic contrast C_o drops to the liminal value. Call this range the daylight visual range V_d. Then, from equation (8) with $R = V_d$ and $C_R = \varepsilon$,

$$V_d = -\frac{1}{\sigma} \ln \left| \frac{\varepsilon}{C_o} \right| \tag{9}$$

The subscript d denotes "daytime."

The definition of V_d given by equation (9) is exact. The practical difficulty of the equation lies in the specification of a working value for ε. The definition of ε involves the consideration of the response of the human eye to light stimuli, and physiological differences alone will preclude complete agreement between any two observers on an exact value for ε. Moreover, the impression of a *single* observer as to what constitutes a liminal contrast value on any given occasion will be dictated not only by his physical health, but also by his mental attitudes of attention or distraction, and the effects of boredom and fatigue (This is the point at which the physiological and psychological factors alluded to in Section II enter into the specification of visual range). Although the exactness or reality of a visual range defined on the basis of a single, specified value for ε might thus be questioned, the utility of the definition remains. That is, the definition does provide a means for indicating the clearness (or otherwise) of the atmosphere in terms of a distance. This fact is, of course, the essence of the use of visual range estimates as measures of air pollution due to particulate loadings.

One of the earliest values offered for ε was by Koschmieder in his pioneer work in 1924 regarding vision through the atmosphere; he made the assumption that for objects of a "reasonable" size, seen in daylight, the liminal contrast is 0.02. Subsequent experimental work both in the laboratory and in the field indicated this value as being rather wide of the mark, though it still persists in the definition of what today is termed the *meteorological range* (*Middleton, 1952*). The recommendations made by Blackwell in 1949 to the Aviation Lighting Committee (*Blackwell, 1949*) are the origin of the currently accepted value $\varepsilon = 0.055$ used by the Federal Aviation Administration (FAA) as the basis for the definition of a daylight visual range (*Federal Aviation Administration, 1968*).

With the value $\varepsilon = 0.055$, and for black objects with $C_o = -1$ (or at least for fairly dark objects with C_o approaching -1), equation (9) may be stated,

$$V_d = \frac{2.9}{\sigma} \tag{10}$$

There is a twofold advantage in the definition of the daylight visual range given by equation (10). First, because it is based on an assumed liminal contrast value of 0.055--the more realistic value relative to the minimum brightness contrast detectable by the "typical" human eye--visual ranges calculated on the basis of equation (10) (given the necessary *a priori* knowledge of σ) will be in better agreement with "visibility" estimates obtained from strictly subjective observations. Second, the bulk of visual range data has been, and is, acquired at local airports under the aegis of the FAA. Thus, the visual range climatology available for comparative and supportive data for specialized visual range measurement programs has developed from data which are also based on the assumed value $\varepsilon = 0.055$.

It should be emphasized that equation (10) holds for "dark" objects of "reasonable" size viewed against the daylight horizon sky. A "reasonable" size would be an object that subtends an angle of from 0.5 to 1.0 degrees of arc from the observer.

NIGHTTIME VISUAL RANGE *

Obviously, nighttime visual range cannot be stated in terms of how far a "dark" object can be seen against the horizon sky; rather, the statement is made in terms of the distance at which a high intensity light source can just be seen. The governing law in this case is Allard's law (*Middleton, 1952*);

$$E = \frac{I}{R^2} e^{-\sigma R} \tag{11}$$

where E is the illuminance (lumens ft^{-2}) established at the range R (ft) by a light of intensity I (candelas). The concern now is not in regard to the *contrast* threshold of the human eye, but rather to the *illuminance* threshold, i.e., to the minimum "amount" of light falling on the eye which produces a recognizable sensation of brightness.

Adopting once more the recommendations of the FAA, the nighttime threshold illuminance is taken as 2 mile-candles (7.17×10^{-8} lumens ft^{-2}). Assuming further a standard light intensity of 10,000 candelas (runway light setting No. 5), equation (11) is written (*Federal Aviation Administration, 1966*),

$$25.43 = 2 \ell n V_n + \sigma V_n \tag{12}$$

where the subscript n denotes "nighttime."

Again, the emphasis is on the fact that the development of equation (12) is according to FAA sanctioned visual range standards. The comparison of equations (10) and (12) illustrate, moreover, the intuitive idea that given the same atmospheric turbidity conditions (as specified by a given σ-value), it is easier to see a bright light at night than it is a dark

* English units are retained in conformance with FAA standards.

object by day (larger absolute values of intrinsic contrasts, cf. equation [5]). That is, *within the context of the accepted day and night visual range standards*, and for a given value of the extinction coefficient, the nighttime visual range is greater than the daytime visual range.

Even during daytime, in fact, it is recognized that under excessively turbid conditions the 10,000 candela light source can be seen at greater distances than can the "dark" object used as the usual reference for the specification of daytime visual range. The FAA specifies the value 1000 mile-candles (3.58×10^{-5} lumens ft $^{-2}$) as the daytime *illuminance* threshold. Using this value, along with the 10,000 candela light intensity, in equation (11), a daytime visual range *relative to the distance the high intensity light source can be seen* is specified by the following equation:

$$19.45 = 2 \ln V_d' + \sigma V_d' \qquad (13)$$

Through the comparison of equations (10) and (13), the question can now be addressed as to what are the daylight conditions under which it is easier to see the light source than it is to see the dark object; i.e., what type of "target" can be seen at the greatest distance? Consider the case when the visual ranges relative to viewing both the light and the dark object are equal. Solving equations (10) and (13) simultaneously for σ for this case ($V_d = V_d'$) yields the value $\sigma = 7.25 \times 10^{-4}$ ft $^{-1}$, and both equations predict a "daylight" visual range of about 4000 feet. For $\sigma > 7.25 \times 10^{-4}$ ft $^{-1}$, i.e., for more turbid atmospheres, $V_d < V_d'$, for relatively "clean" atmospheres ($\sigma < 7.25 \times 10^{-4}$ ft $^{-1}$), $V_d > V_d'$. In other words, in clean air a dark object against the horizon sky can be seen and recognized at greater distances than the bright light, and *vice versa*. This fact is recognized by the FAA in airport operations. That is, when the daytime visual range defined in reference to viewing a dark object against the horizon sky (equation [10]) drops to 4000 feet, the high intensity runway lights are turned on as an aid to air traffic movement, and "daytime" visual ranges are subsequently specified relative to the distance at which those lights can be seen.

THE STANDARD DAY-AND NIGHTTIME VISUAL RANGES

Shown plotted in Figure 1 are the day- and nighttime visual ranges defined by equations (10), (12), and (13), as functions of the atmospheric light extinction coefficient. The dash-dot and solid lines are for nighttime and daytime visual ranges, respectively. The break in the daytime curve at a visual range of about 4000 feet reflects the fact that daytime visual ranges less than 4000 feet are *defined* relative to the distance at which the standard light source can be seen (equation [13]); for ranges greater than 4000 feet, the definition is relative to the "dark object" target (equation [10]). By way of interest, the dashed line is the "meteorological range" versus σ curve, i.e., the "daytime" visual range based on Koschmieder's value for the liminal contrast $\varepsilon = 0.02$.

The crossover of the day- and nighttime curves at a visual range value of about 16 miles is a consequence of the difference between Duntley's law (equation [8]) and Allard's law (equation [11]). That is, the decay of contrast with distance is only according to atmospheric transmittance (the exponential term in equation [8]). Compounding this effect relative to a point light source, however, is the purely *geometrical* effect of the "R^2-loss" on received intensity. At large ranges, the R^2-loss is indeed the dominant effect.

It is to be emphasized that the visual range curves in Figure 1 are based on the visual range standards as defined by the FAA. *These curves thus constitute the basis for interpreting all available visual range data from airport operations in terms of the optical quality of the atmosphere.*

THE MEASUREMENT OF VISUAL RANGE

Instruments to measure visual range may be separated into two broad categories: those instruments that measure contrasts between "targets" and backgrounds directly, and those that measure σ, with the subsequent interpretation of the measurements in terms of visual range according to the relationships shown in Figure 1. Consider first the contrast-measuring instruments.

TELEPHOTOMETERS

Visual range instruments that measure contrasts, i.e., compare brightnesses, are in principle comparison telephotometers. One class of such instruments compares the luminance of a distant source with that of a comparison source in the telephotometer. The other measures only the *relative* luminance of two distant sources, as, for example, a large dark building and the horizon sky above it. The former class of telephotometer is best suited for visual range measurements at night (comparison of the brightness of a distant "point" source of light with that of an internal point source, e.g., as with Middleton's "artificial star" telephotometer [*Middleton, 1932*]). Measurement of the relative luminances of distant objects are best suited for daytime use.

Actually, to measure the visual range when the target is at a distance $R < V_d$, all comparison telephotometers are "calibrated" according to equation (8) written in a slightly different form. For $R < V_d$, and for black objects viewed against the horizon sky,

$$\sigma = \frac{1}{R} \ln \left| \frac{1}{C_R} \right| . \qquad (14)$$

Substituting equation (14) into equation (10),

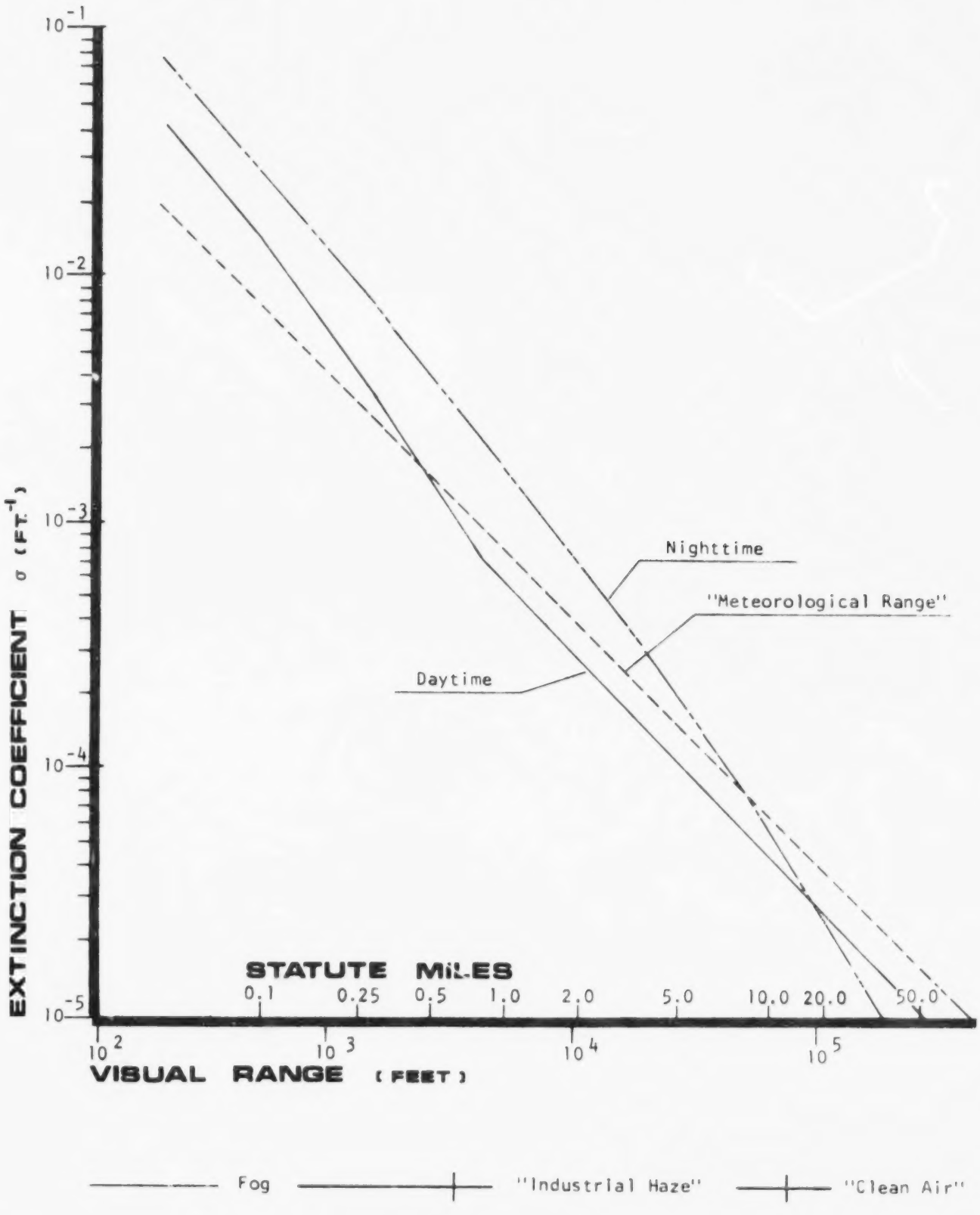

Figure 1: Day- and nighttime visual ranges, defined according to the FAA visual range standards, versus the atmospheric extinction coefficient.

$$V_d = \frac{2.9R}{\ell n \left| \frac{1}{C_R} \right|} . \qquad (15)$$

It is the apparent contrast,

$$C_R = \frac{B_R - B_h}{B_h} , \qquad (16)$$

where B_h is the brightness of the horizon sky, that is measured with such instruments. For strictly optical instruments, the "measurement" is a subjective estimate by the viewer as to when the brightness of the target is "matched" (by insertion of calibrated filters) to that of the horizon sky. Electrooptical instruments eliminate this subjectivity by measurement of the brightness of the target and horizon independently.

EXTINCTION MEASUREMENTS

Again, two general classes of instruments may be defined that measure the atmospheric extinction coefficient directly. The first type of instrument yields σ-data from a measurement of transmittance; the second type measures σ directly by sampling a small volume of air, with the assumption that the remaining atmosphere through which the visual range would be determined exhibits spatial homogeneity. Consider first the measurement of transmittance.

TRANSMISSOMETER

The Bouguer-Lambert law is the basis for σ-estimates from transmittance measurements; i.e., equation (3) may be written,

$$\sigma = - \frac{\ell n \, \tau}{R} \qquad (17)$$

Given a light source of known, intrinsic intensity I_o located a distance R = B from a receiver, then from the definition of transmittance simply as the ratio of received to intrinsic source intensities, the transmissometer yields σ-data according to,

$$\sigma = - \frac{(\ell n \, I - \ell n \, I_o)}{B} , \qquad (18)$$

when B is the transmissometer basline distance, i.e., the distance separating source and receiver. The σ-estimates so obtained can then be used in equations (10), (12) or (13) for the appropriate specifications of the day- or nighttime visual ranges.

INTEGRATING NEPHELOMETERS

An alternate approach to the direct measurement of σ is through use of an instrument termed the integrating nephelometer. The principle upon which the instrument is based is the fact that when an elementary aerosol volume is illuminated by parallel light, light will be scattered from the illuminating beam in all directions. Clearly in the absence of absorption (i.e., $\sigma = k_s$, cf. eg. (2)) the total flux scattered in all directions equals the incident flux. The summation of this flux over the sphere enclosing the (unit) scattering volume gives the scattering extinction coefficient; i.e.,

$$k_s = \int_v \frac{I(\phi)}{E} dv, \tag{19}$$

where $I(\phi)$ is the intensity of the elemental volume as seen in the direction ϕ, E is the beam illuminance, and the integration is over the sphere enclosing the volume. The integrated flux measurement is the measurement performed by the integrating nephelometer. Again, substitution of the σ-values measured by the nephelometer into equations (10), (12), or (13) defines the appropriate visual ranges.

SECTION V

FIELD TEST RESULTS

GENERAL

The three month field test program required the measurement of visibility related parameters using the following techniques and instruments:

1) One trained observer for estimating the average visible range around the horizon;

2) One telephotometer for measuring the reduction in contrast of dark objects against the horizon sky at varying distances and in four directions equally spaced around the horizon;

3) One transmissometer for measuring the attenuation of a light beam transmitted through the atmosphere; and,

4) Two integrating nephelometers for measuring the light scattering from atmospheric aerosols. One, stationary and operated in close proximity to the transmissometer, the other portable and used to determine the amount of local inhomogeneity in the light scattering properties of the atmosphere.

DATA ACQUISITION SITE

As shown in Figures 2 and 3 the sampling site was located on the floor of the Green River Valley, about 3.2 km southeast of Seattle-Tacoma International Airport, and 10 km south of Boeing Field. Close proximity to Boeing Field and the Sea-Tac Airport and the "funneling" effect of the valley on pollutants from the industrialized Duwamish River Valley to the north were factors which favored the selection of the sampling site.

Although from several aspects the measuring site was less than ideal for optimal scientific results, actual measuring conditions were perhaps typical of a practical site that would be used by a local agency and, at times, reflected circumstances in an industrialized river valley.

The selection of the site for the conduct of the proposed program was governed in part by the following set of criteria:

1) The site was to be located where a suitable range of visibilities would occur during the prescribed two-month measurement period;

2) The site was to be located in an area where an air quality authority maintains appropriate sampling equipment;

3) The site was to be located within reasonable distance from one or more airports to make use of FAA visibility data;

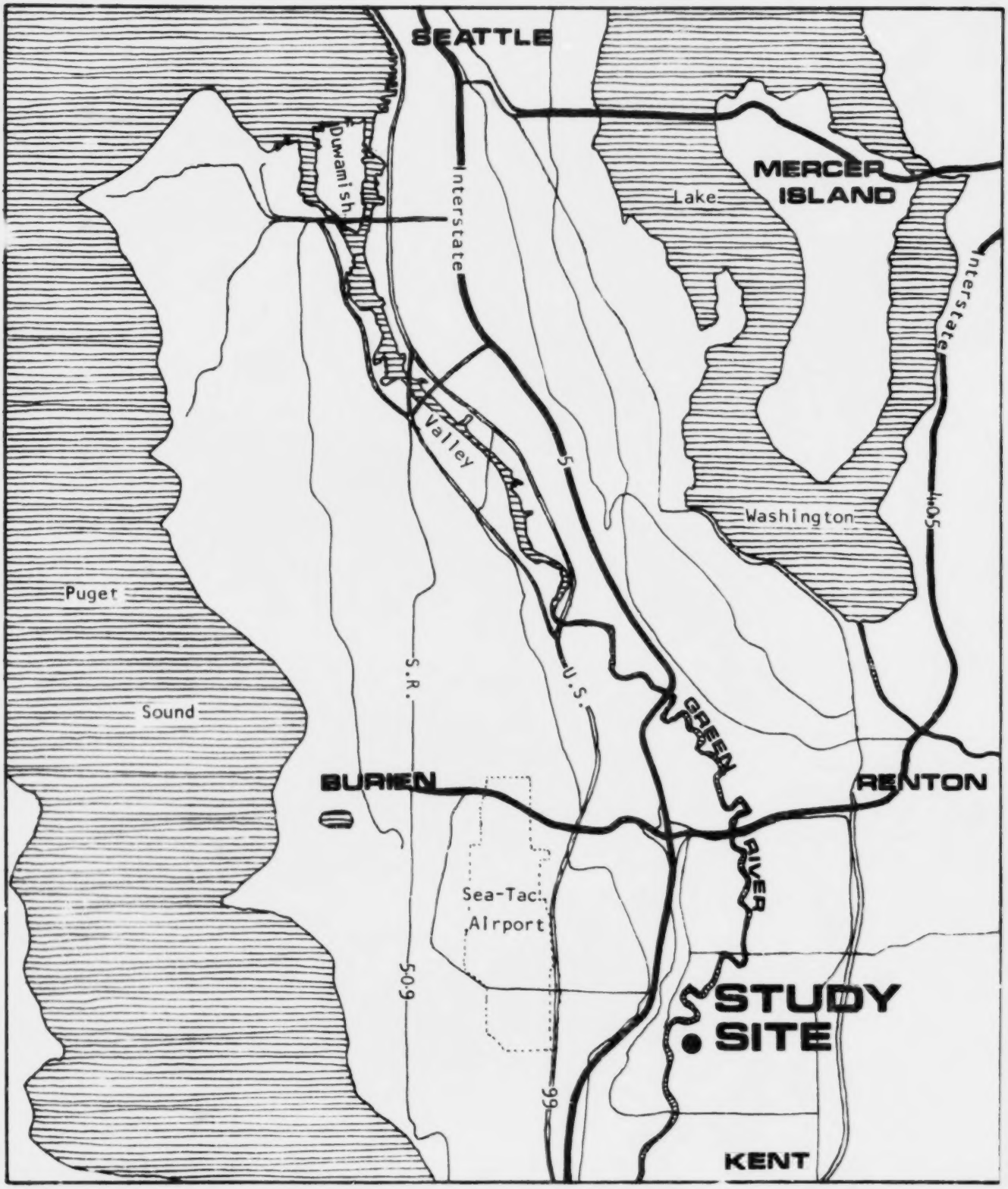

Figure 2 Regional location of study site.

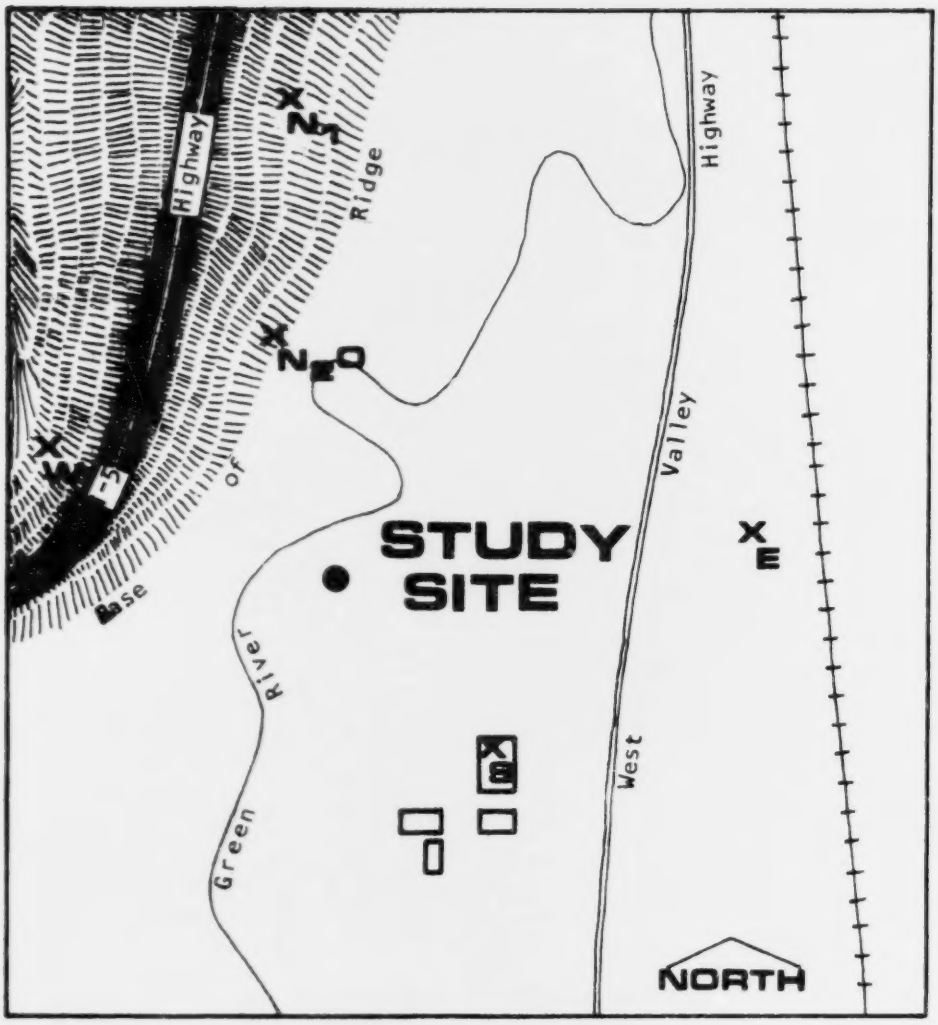

O Transmissometer Retroreflector

X Telephotometer Targets

Scale: ⊢——1 km——⊣

Figure 3: Local scale site map showing target locations.

4) The site was to be located where topography permits the necessary range for target objects to be viewed;

5) The site was to be located where suitable horizon level "dark" objects were available.

MEASUREMENT PROCEDURES

VISUAL ESTIMATIONS

A trained observer, using remote visual targets at known distances (a large variety of natural and man-made targets at ranges from about 1/2 km to greater than 50 km), estimated prevailing visibility for quadrants primarily to the north and south. Due to limited horizontal sight paths to the east and west, observations in these directions were restricted to low visibilities. Visual targets were selected based upon guidelines presented in (*Middleton*, 1952). Observations were taken every three hours at approximately the same time at which the airport visibility estimates are made, and the recorded prevailing visibilities represent the average value from all quadrants. The trained observer did not view the readouts of the instruments.

TELEPHOTOMETER MEASUREMENTS

Telephotometer measurements employed the Gamma Scientific 1C2000 telephotometer which is a manually operated instrument. It consists of a focused aperature optical head and sensing photomultiplier. The photomultiplier "sees" through a photopic correction filter which adjusts the spectral sensitivity of the instrument to that of the human eye. Luminance measurements of a remotely located visual target and its background horizon to obtain a light contrast ratio were made and manually recorded.

In utilizing the 1C2000 telephotometer, the target and background instantaneous luminance values were obtained. From these data, the contrast ratio, extinction coefficient and visual range were determined using equations (4), (7) and (8), respectively, discussed in Section II. These observations were confined to daytime observations since luminance measurements taken from a passive target require a minimum level of ambient light.

Table 1 and Figure 3 summarize the location and nature of the targets utilized in the telephotometer measurements. Measurements in the northern sector were made using man-made targets at ranges of 0.82 and 1.58 km which were comprised of large "black boxes" with central holes of 0.8 m and 1.6 m diameter, respectively. These targets were cubic, painted flat black within, and at the 0.82 km and 1.58 km ranges were 1.6 m and 2.4 m on a side, respectively.

The target to the west consisted of a flat black-painted surface located near the base of a ridge at 1.2 km from the central site. The target in the south quadrant was a large parabolic antenna located atop a building in the Boeing Kent Aerospace complex. To the east, a large water tower served as a target. Both the parabolic antenna and the water tower were painted flat black and subtended angles of greater than six minutes.

TABLE I

TELEPHOTOMETER TARGET DATA

Target Location as Shown in Figure 2	Range from Central Site, (Meters)	Angular Separation Between Target and Sky Background, (Degrees)	Angular Size of Target (Minutes)
N_1	1.58 km	0°	5.3
N_2	0.82 km	3°	6.4
E	1.40 km	1°	>6
S	0.88 km	0°	>6
W	1.19 km	0°	4.4

TRANSMISSOMETER MEASUREMENTS

The NETL 63TI laser transmissometer was employed to determine extinction coefficients as measured over the round trip distance between the laser source and retroreflector. The retroreflector was located in the northern quadrant 820 m from the central measuring site in close proximity to one of the telephotometer targets as shown in the field site location map given in Figure 3. Transmissometer output measurements are linearly related to the extinction coefficient. Reduction of these measurements to prevailing visibility was accomplished using equation (10) discussed in Section IV.

Primary calibration was performed during initial equipment installation. Further calibration checks were performed automatically by the periodic insertion of a neutral density filter into the receiving system. Strip chart records thereby provided a history of the calibration response in addition to measured extinction coefficients.

Initial transmissometer measurements involved manually positioning the transceiver mount which was adjustable in azimuth and elevation. Early in the study it became apparent that an elevation adjustment was necessary for each three-hour observation in order to recover the maximum return signal from the retroreflector. A series of tests indicated that pointing errors occurred which were apparently associated with temperature changes in the transmissometer mount and/or refractive beam bending effects. To facilitate automatic recording and minimize human error, a scanning motor was incorporated which cycles the elevation pointing angle in a period of approximately 40 minutes. This autoscan time

interval increased the minimum time between successive transmissometer measurements to about 40 minutes.

The retroreflector assembly was comprised of two 2.54 cm corner cube reflectors and one 6.35 cm corner cube reflector mounted within a 12 cm diameter tube.

The beam divergence of the laser was about one milliradian and the exit beam diameter from the transceiver is approximately 0.8 millimeters. The receiving aperature at the transceiver was 7.5 cm. Consequently, a relatively small fraction of the total transmitted signal is collected by the transceiver receiver optics.

NEPHELOMETER MEASUREMENTS

Meteorology Research, Incorporated (MRI) Model 1550 integrating nephelometers were used to provide measurements of the scattering coefficient at the central receiving site and at varied locations in the nearby vicinity. Normal operation of the nephelometer involved setting the flash interval to 4 seconds, setting the averaging time to 100 seconds, and setting the measurement range to the 4.8 km to ∞ scale.

Calibration of the nephelometer was routinely performed using a primary standard consisting of particle-free air for the zero adjustment and particle-free freon gas for the upscale calibration point.

The Model 1550 nephelometer is a compact, relatively portable instrument requiring a minimum of special installation considerations. The measurement module which was located inside a mobile van for the portable measurements and inside a trailer for the measurements at the central site location.

During the course of the field measurement program an attempt was made to maintain the inside temperature of the instrumentation trailer at the outside ambient temperature. The reason for this precaution was to minimize temperature differences that might have been experienced by an air sample in transit to the nephelometer. A temperature difference will produce a relative humidity difference between that of the ambient air and that of the sampling volume. Consequent variations in the moisture content of hygroscopic nuclei could introduce inaccuracies in the determination of meteorological range.

To investigate the dependence of measured scattering on a variation in the moisture content of hygroscopic nuclei, a cyclicly operated heater was employed internal to the inlet air sampling hose of the nephelometer. The heater completed one cycle per hour over an operation period of approximately two months. However, nephelometer data, unless otherwise specified in this report, corresponds to operating conditions with the inlet heater off.

The importance of operating the nephelometer at the ambient outside temperature for relative humidities exceeding 80 percent is illustrated by data presented in Figure 4 which was obtained during the temperature

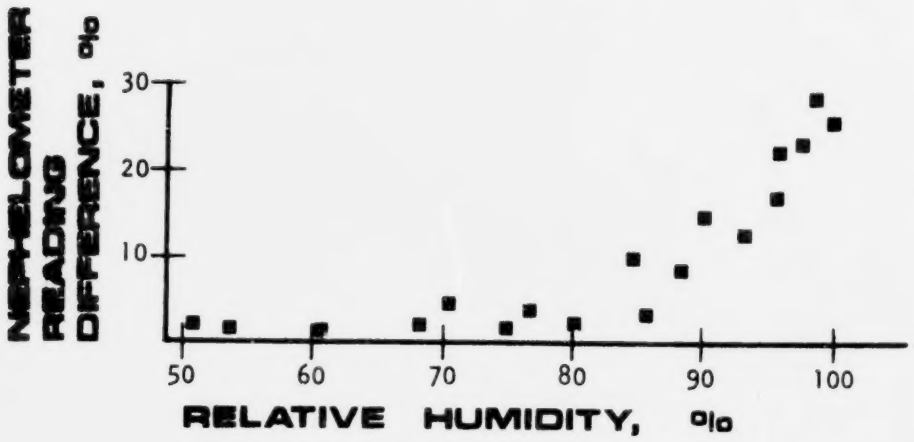

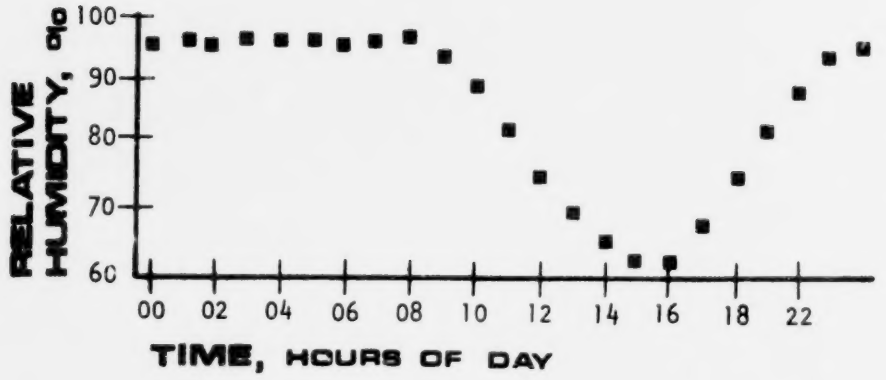

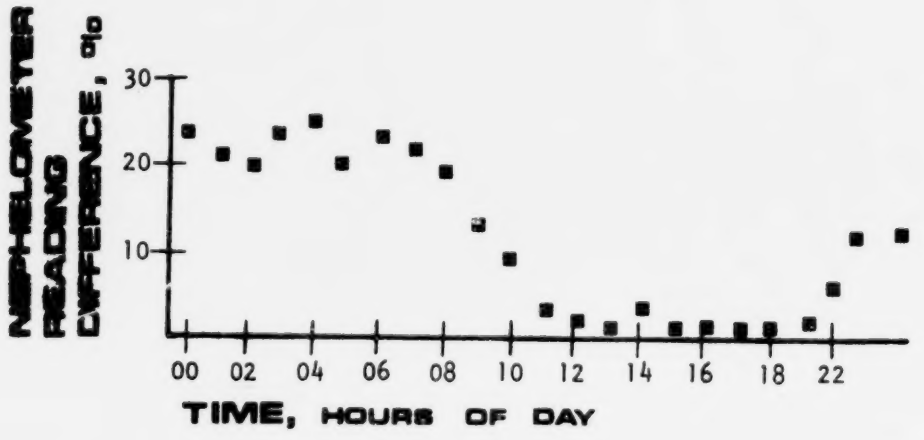

Figure 4: Nephelometer-humidity difference relationships.

cycling. From this figure, it is evident that as the relative humidity approaches 100 percent, b_{scat} differs by nearly 30 percent from the readings obtained with the inlet heater on. During the course of the temperature cycling, data were selected on the basis of high-humidity days which formed the basis for the results shown in Figure 4.

WAVELENGTH CONSIDERATIONS

Each measuring instrument has an associated bandwidth and central wavelength. For example, the telephotometer has a spectral response very similar to the visual response nerve of a "typical" human eye, i.e., a central wavelength of about 550 nanometers and an effective bandwidth of about 150 nanometers. The integrating nephelometer has an irregular spectral response curve of halfwidth about 150 nanometers. The output of the nephelometer is referred to a wavelength of 460 nanometers. Primary response of the tranmissometer is to a nearly monochromatic laser beam at 633 nanometers. Any specific human observer will also have a visual response different from the "typical" human, and will be afflicted by psychovisual interferences. Each method of determining visibility will therefore be subject to "correction" factors related to spectral response. Application of invariant wavelength correction factors will act to reduce bias and may reduce scatter in the observations. Wavelength correction factors were not utilized in this study.

MEASUREMENTS AT THE CENTRAL SITE

An instrumentation van was located at the central field measuring site. At this site strip chart recordings were taken of dewpoint, outdoor temperature, windspeed, wind direction, scattering coefficient (nephelometer), and extinction coefficient (transmissometer). Tabulated values of visibility parameters related to the human observer, airport-reported prevailing visibility, nephelometer, time averaged nephelometer, transmissometer, and telephotometer observations and relative humidity throughout the observing period from August 9, 1973 to October 17, 1973 are given in Appendix B.

EXPERIMENTAL RESULTS

GENERAL

During the period of field measurements, 150 sets of data were taken of which 67 correspond to relative humidities less than 70 percent.

Local observer and airport visibility values are given in terms of range, i.e. kilometers. In accordance with contract requirements, the nephelometer results are reported in terms of scattering coefficients, and the transmissometer and telephotometer results are reported in terms of extinction coefficient, as defined by H. Horvath and I.E. Noll (*1969*). Coincident with the visibility related parameters are listed relative humidity and outdoor temperature as measured with E G & G Model 880 dewpoint hygrometer instruments.

Also included in Appendix D are the test results from the roving nephelometer which provided 49 sets of measurements at the central receiving site and 40 sets in the nearby vicinity over the interim of the field test program. The majority of measurements taken with the roving unit were at times when the relative humidity was less than 70 percent.

Tabulated airport visibility is composed of an average of the visibilities at Boeing Field and Seattle-Tacoma International Airport.

Daily observations began at 0900 and continued at three-hour intervals. The normal observation schedule usually allowed the completion of four observational sets each day. Observations were normally suspended during rain or extremely clear weather.

During the course of the data collection program, relative humidity varied from 35 to 100 percent and weather conditions varied from bright, clear days to heavy fog or strong haze. Maximum daily ambient temperatures varied from 40 degrees F to over 80 degrees F.

SUSPENDED PARTICULATES

Using equipment and personnel of the University of Washington, limited suspended particulate sampling was initiated at the site on August 11, 1973. Data was collected for 13 days and reduced to yield daily averages. Beginning on October 9, 1973, particulate sampling was resumed for a duration of seven days using equipment supplied by the U.S. Environmental Protection Agency, Region X. Average daily loadings were light during the sampling periods (7 to 55 microgram per cubic meters) and reflect as relatively low levels of suspended particulate in the Green River Basin relative to that of the Duwamish River Basin in South Seattle.

Additional mass loadings for the times of interest were obtained from the Puget Sound Air Pollution Control Agency ambient air monitoring station which was located approximately on a ridge two miles west of the central field measuring site. These data are also summarized in Appendix D.

PHOTOGRAPHS

Seventy-nine color photographs of the north and south horizons were taken during many observation periods. In addition, the horizon panorama surrounding the site was photographed. These photographs are included under separate cover as a supplement to this report (private communication, Thomas Dzubay, 1974).

CORRELATION COEFFICIENTS BETWEEN PAIRS OF MEASUREMENT METHODS

Correlation coefficients between pairs of measuring methods were determined from the data summarized in Appendix B. Using a CDC 6400 computer and the Statistical Package from the Social Sciences Program (*Nie, et al.*, 1970), correlation coefficients were determined for measurement data pairs of linearly related visibility parameters (cf. eqs. (20) and (21)).

Accordingly, correlation coefficients were determined between the natural logarithm of the prevailing visibility (airport or local observer) and the natural logarithm of instrument derived light extinction or light scattering coefficient. Additionally, correlation coefficients were determined between the airport or local observer reported prevailing visibility and the instrument derived visual range. Conversion of the instrument-determined visibility parameters to visual range was accomplished in accordance with the procedures discussed in Section IV.

Correlation coefficients between pairs of measurement methods, utilizing 144 sets of measurements (6 sets less than the 150 total because time averaging of six nephelometer readings could not be performed), are summarized in Table 2. The coefficients are tabulated by relative humidity ranges of 0-65, 0-80, 0-90 and 0-100 percent respectively.

Visibility related measurements were segregated in accordance to the local prevailing visibility range and the resulting correlation between measurement methods are presented in Table 3. These data correspond to visibility ranges of 0 to 8 km, 8.1 to 16.1 km, 16.2 to 24.2 km and ranges exceeding 24.2 km respectively. (All 150 sets of data pairs are used because the time average nephelometer was not included in this comparison.)

All instrument and observer estimates of visibility were expressed in forms that were expected to be linearly related (i.e., prevailing visibility versus meteorological range or the common logarithm of prevailing visibility versus the common logarithm of extinction or scattering coefficient). Prevailing visibility versus meteorolgical range correlation coefficients are in the lower left portions of Table 2 and 3. Correlation coefficients for the natural lagarithm of prevailing visibility versus the natural logarithm of extinction or scatter coefficients are in the upper right hand portion of Tables 2 and 3.

Caution must be exercised in the interpretation of the correlation results because the degree of confidence is dependent on the number of sets of data available. Ninety-five percent confidence intervals corresponding to the correlation coefficients are presented in Figure 5. These confidence intervals apply to 150 measured data pairs and do not include the time averaged nephelometer. For smaller numbers of data pairs the confidence limits will according to increase.

SCATTERGRAMS

Figures 6 - 10 are scattergrams developed from the data in Appendix B. Commensurate with the purpose of the field test program, the central dashed lines in the figures represent the linear lines of regression of observer estimated visibilities on instrument derived visibilities,

$$V_{obs} = a + bV_{inst}; \tag{20}$$

that is, in eq. (20), instrument-derived visibilities are considered the predictors, and the observer visibilities the predictands. The dashed lines bracketing the regression lines mark the scatter (one standard deviation) in the data pairs; i.e., in each figure about 68 percent of the observations fall between the two scatter lines. The statistics of the

TABLE 2

CORRELATION COEFFICIENTS FOR RELATIVE HUMIDITY RANGES

(a) 0 - 65 percent relative humidity

	OBS	APVIS	INST NEPH	1-Hour Avg. NEPH	TRANS	TELE
OBS	1.00	0.61*	-0.54*	-0.60*	-0.13*	-0.62*
APVIS	0.61	1.00	-0.51*	-0.55*	00.13*	-0.44*
INST NEPH	0.64	0.51	1.00	0.89*	0.10*	0.71*
1-Hour Average NEPH	0.64	0.52	0.90	1.00	0.09*	0.71*
TRANS	0.09	0.18	0.18	0.13	1.00	0.30*
TELE	0.69	0.53	0.79	0.75	0.22	1.00

Number of observations = 55

Legend:

OBS =Observer Estimate
APVIS =Airport Estimate
INST NEPH =Instantaneous Nephelometer Measurement
1-Hour Average NEPH =Time Averaged Nephelometer Measurement
TRANS =Transmissometer Measurement
TELE =Telephotometer Measurement

Starred data denote correlations between $\ln V_i$ and $\ln V_j$.
Unstarred data denote correlation between V_i and V_j.

TABLE 2 (cont.)

CORRELATION COEFFICIENTS FOR RELATIVE HUMDITY RANGES

(b) 0 - 80 percent relative humidity

	OBS	APVIS	INST NEPH	1-Hour Avg. NEPH	TRANS	TELE
OBS	1.00	0.65*	-0.65*	-0.69*	-0.30*	-0.71*
APVIS	0.75	1.00	-0.57*	-0.59*	-0.27*	-0.57*
INST NEPH	0.74	0.68	1.00	0.89*	0.26*	0.75*
1-Hour Average NEPH	0.73	0.66	0.91	1.00	0.22*	0.72*
TRANS	0.43	0.38	0.41	0.39	1.00	0.42*
TELE	0.76	0.70	0.83	0.80	0.50	1.00

Number of observations = 98

Legend:

OBS =Observer Estimate
APVIS =Airport Estimate
INST NEPH =Instantaneous Nephelometer Measurement
1-Hour Average NEPH =Time averaged Nephelometer Measurement
TRANS =Transmissometer Measurement
TELE =Telephotometer Measurement

Starred date denote correlations between $\ln V_i$ and $\ln V_j$
Unstarred data denote correlation between V_i and V_j

TABLE 2 (cont.)

CORRELATION COEFFICIENTS FOR RELATIVE HUMIDITY RANGES

(c) 0 - 90 percent relative humidity

	OBS	APVIS	INST NEPH	1-Hour Avg. NEPH	TRANS	TELE
OBS	1.00	0.70*	-0.59	-0.60*	-0.33*	-0.80*
APVIS	0.62	1.00	-0.52*	-0.50*	-0.36*	-0.61*
INST NEPH	0.59	0.56	1.00	0.90*	0.22*	0.73*
1-Hour Average NEPH	0.63	0.49	0.91	1.00	0.16*	0.70*
TRANS	0.31	0.41	0.31	0.27	1.00	0.39*
TELE	0.88	0.59	0.74	0.77	0.36	1.00

Number of observations = 117

Legend:

OBS = Observer Estimate
APVIS = Airport Estimate
INST NEPH = Instantaneous Nephelometer Measurement
1-Hour Average NEPH = Time Averaged Nephelometer Measurement
TRANS = Transmissometer Measurement
TELE = Telephotometer Measurement

Starred data denote correlations between $\ln V_i$ and $\ln V_j$
Unstarred data denote correlations between V_i and V_j

TABLE 2 (cont.)

CORRELATION COEFFICIENTS FOR RELATIVE HUMIDITY RANGES

(d) 0 - 100 percent relative humidity

	OBS	APVIS	INST NEPH	1-Hour Avg. NEPH	TRANS	TELE
OBS	1.00	0.75*	-0.50*	-0.47*	-0.45*	-0.88*
APVIS	0.57	1.00	-0.46*	-0.41*	-0.44*	-0.68*
INST NEPH	0.22	0.26	1.00	0.91*	0.22*	0.64*
1-Hour Average NEPH	0.22	0.22	0.91	1.00	0.15	0.57*
TRANS	0.44	0.35	0.33	0.25	1.00	0.49*
TELE	0.95	0.58	0.39	0.37	0.60	1.00

Number of observations = 144

Legend:

OBS = Observer Estimate
APVIS = Airport Estimate
INST NEPH = Instantaneous Nephelometer Measurement
1-Hour Average NEPH = Time Averaged Nephelometer Measurement
TRANS = Transmissometer Measurement
TELE = Telephotometer Measurement

Starred data denote correlations between $\ln V_i$ and $\ln V_j$
Unstarred data denote correlations between V_i and V_j

TABLE 3

CORRELATION COEFFICIENTS FOR VISUAL RANGES

(a) 0-8.0 km prevailing visibility

	Obs	Apvis	Neph	Trans	Tele	Rh
Obs	1.00	0.60*	-0.27*	-0.44*	-0.88*	-0.33*
Apvis	0.49	1.00	-0.20*	-0.22*	-0.52*	-0.38*
Neph	0.34	0.08	1.00	0.25*	0.40*	-0.30*
Trans	0.35	0.11	0.15	1.00	0.59*	0.52*
Tele	0.83	0.40	0.29	0.57	1.00	0.33*

number of observations = 17

(b) 8.1-16.1 km prevailing visibility

	Obs	Apvis	Neph	Trans	Tele	Rh
Obs	1.00	0.45*	-0.33*	-0.31*	-0.68*	-0.41*
Apvis	0.29	1.00	-0.31*	-0.22*	-0.46*	-0.49*
Neph	0.30	0.26	1.00	0.04*	0.68*	0.06*
Trans	0.13	0.11	0.00	1.00	0.27*	0.47*
Tele	0.63	0.40	0.70	0.27	1.00	0.21*

number of observations = 54

Legend:

Obs =Observer estimate
Apvis =Airport estimate
Neph =Nephelometer measurement
Trans =Transmissometer measurement
Tele =Telephotometer measurement
Rh =Relative humidity

Starred data denote correlations between $\ln V_i$ and $\ln V_j$
Unstarred data denote correlations between V_i and V_j

TABLE 3 (Continued)

CORRELATION COEFFICIENTS FOR VISUAL RANGES

(c) 16.2-24.2 km prevailing visibility

	Obs	Apvis	Neph	Trans	Tele	Rh
Obs	1.00	0.39*	-0.32*	0.04*	-0.31*	-0.03*
Apvis	0.30	1.00	0.04*	-0.18*	-0.04*	-0.35*
Neph	0.24	-0.07	1.00	-0.21*	0.45*	-0.35*
Trans	0.04	0.09	-0.12	1.00	0.11*	0.19*
Tele	0.27	-0.01	0.44	0.22	1.00	-0.10*

number of observations = 60

(d) Greater than 24.2 km prevailing visibility

	Obs	Apvis	Neph	Trans	Tele	Rh
Obs	1.00	0.29*	0.13*	-0.04*	0.12*	-0.05*
Apvis	0.25	1.00	-0.24*	-0.20*	0.06*	-0.61*
Neph	-0.22	0.29	1.00	0.24*	0.72*	0.33*
Trans	-0.11	0.22	0.04	1.00	0.46*	0.15*
Tele	-0.15	-0.07	0.62	0.07	1.00	0.14*

number of observations = 19

Legend:

Obs =Observer estimate
Apvis =Airport estimate
Neph =Nephelometer measurement
Trans =Transmissometer measurement
Tele =Telephotometer measurement
Rh =Relative humidity

Starred data denote correlations between $\ln V_i$ and $\ln V_j$
Unstarred data denote correlations between V_i and V_j

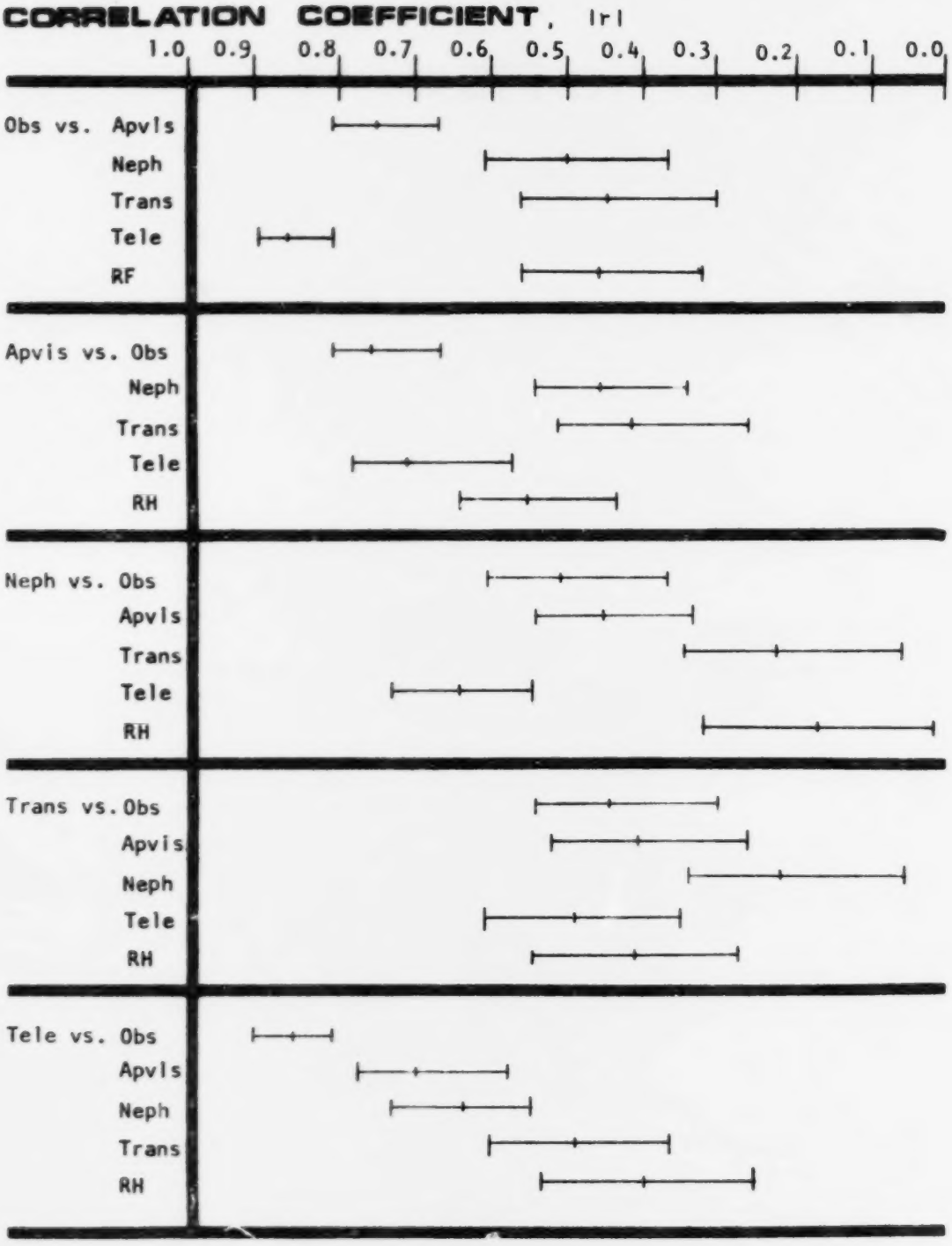

Figure 5: Correlation coefficients and 95% confidence limits for lnV versus lnσ.
(all observations, n=150)

regression analyses shown in the Figures are given in Table 4. Included in the table are the linear regression coefficients [a and b, eq. (20)], the scatter (rms deviations of observed from predicted observer visibilities), and the coefficients of linear correlation of the data pairs.

From the data shown in Figures 6 - 10 and given in Table 4, the telephotometer clearly emerges as the best instrument for visibility estimates. That is, in the relationships between observer and instrument-derived visibilities, the scatter is least, the correlation the highest, and the "zero-offset (the magnitude of a, eq. (20))" the least in the telephotometer data. Overall analytical results are similar for the nephelometer and transmissometer (Table 4).

Figures 11-15 are scattergrams developed from the common logarithms of the data in Appendix B. The central dashed lines again represent the linear lines of regression, but in each case for the specified visibility method (vm) against the telephotometer,

$$\text{Log } \sigma_{vm} = a + b \text{ Log } \sigma_{tele} \tag{21}$$

that is, in eq. (21), the extinction coefficients derived for the telephotometer method are considered the predictors and the extinction coefficients derived from the other methods are the predictands. The dashed lines bracketing the regression lines are again the one-sigma scatter and the circled data points are those points corresponding to conditions when relative humidity exceeded 80 percent. Statistics of the regression analysis are given in Table 5.

From the data shown in Figures 11 - 15 and given in Table 5, the local observer against the telephotometer clearly reflects the previous conclusion drawn from comparisons of the direct variables. The instrument which exhibited the highest correlation, smallest intercept value, and regression line slope nearest unity was the instantaneous nephelometer, although the time averaged nephelometer exhibited the least scatter. These results indicate that there was little gained by time averaging. The transmissometer data proved to have the lowest correlation and largest scatter of all methods, although the slope of their regression line was nearest to unity and displayed an insignificant bias. An important conclusion regarding these rather inconsistant results is that a substantially larger sample size should be utilized in future studies.

RMS FRACTIONAL DEVIATION

As a further indicator of the relationship between the telephotometer and other methods for determining visibility the rms fractional deviation (d) has been calculated for the various humidity ranges. This parameter is defined as

$$d = \left[\frac{\sum_i \left(\frac{x_i - y_i}{y_i} \right)^2}{N} \right]^{\frac{1}{2}} , \tag{22}$$

where y_i are the telephotometer measurements, x_i are the measurementments by other methods, and N is the total number of measurement pairs. In the

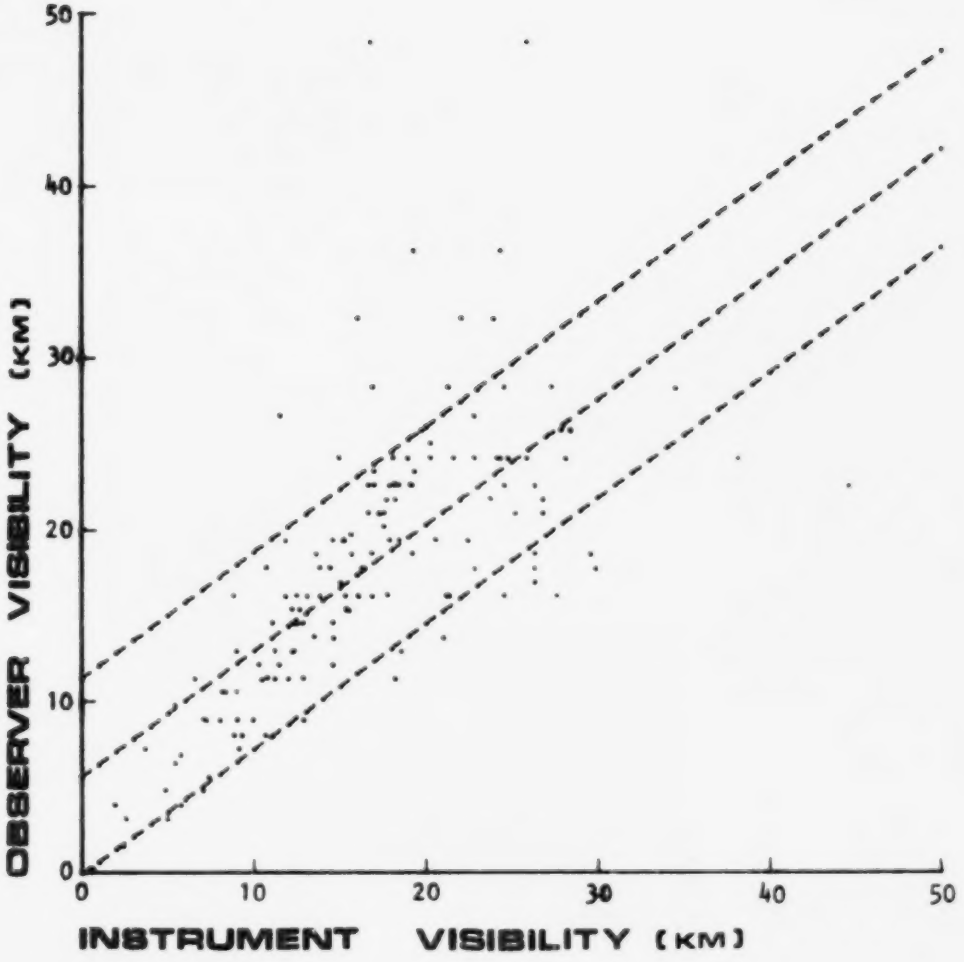

Figure 6: Scattergram for observer visibility versus instrument visibility (telephotometer)

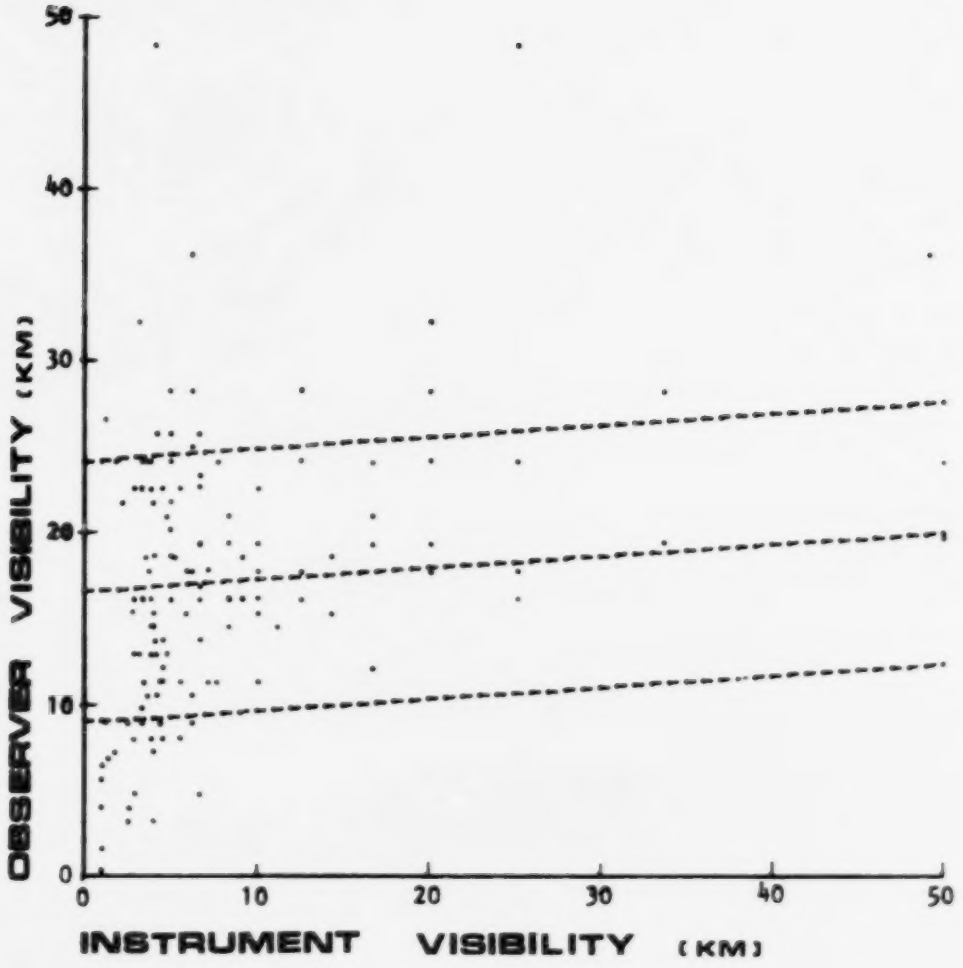

Figure 7: Scattergram for observer visibility versus instrument visibility (transmissometer)

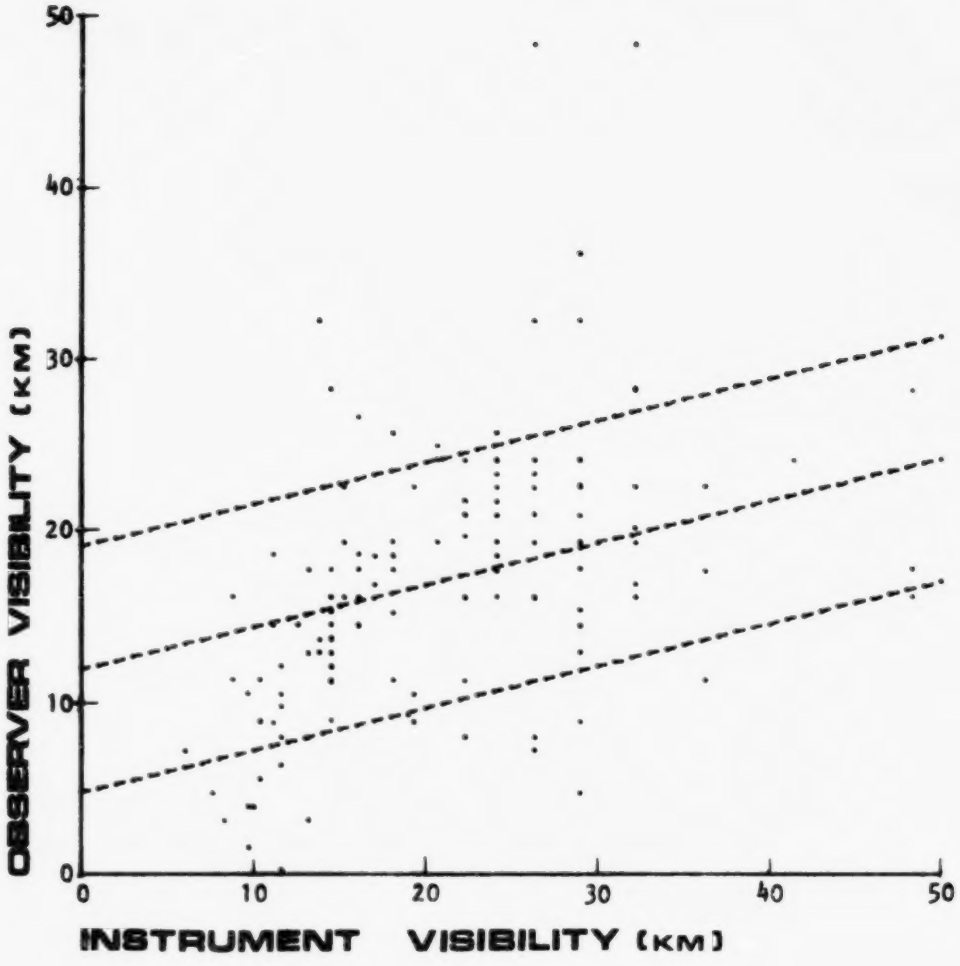

Figure 8: Scattergram for observer visibility versus instrument visibility (nephelometer)

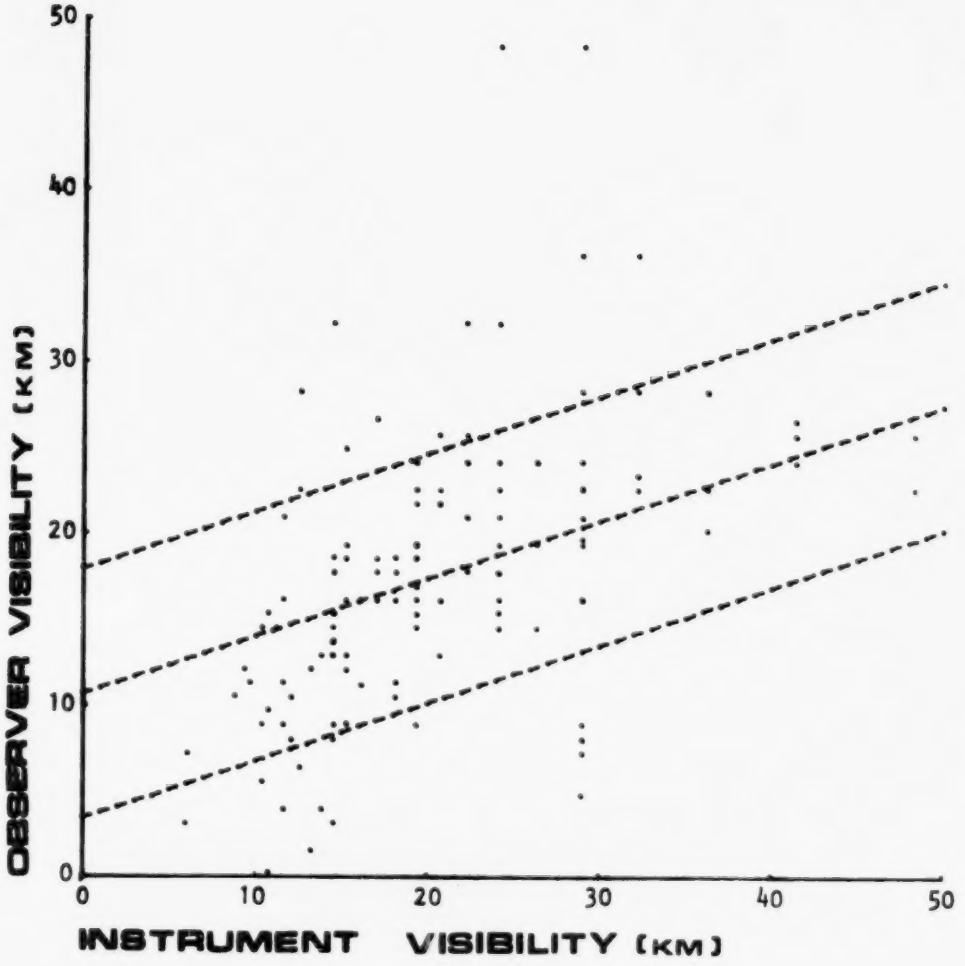

Figure 9: Scattergram for observer visibility versus instrument visibility (averaged nephelometer)

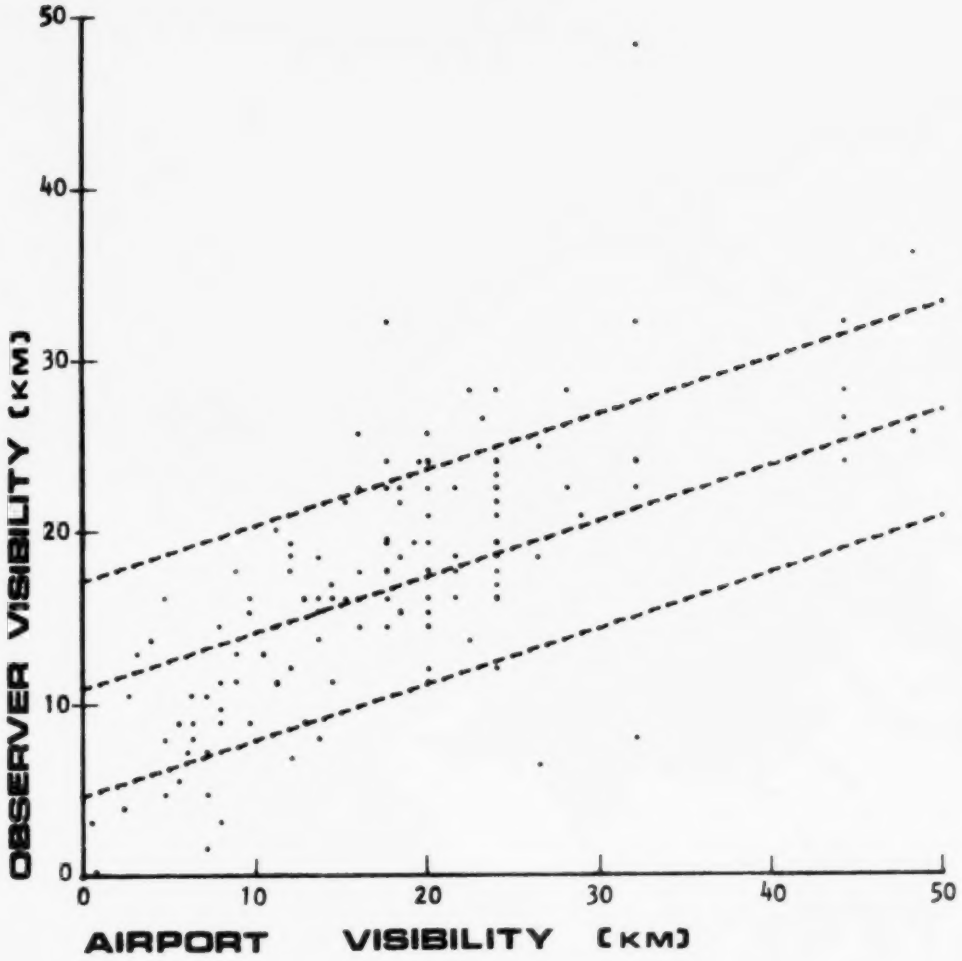

Figure 10: Scattergram for observer visibility versus airport visibility

TABLE 4

SUMMARY OF REGRESSION ANALYSIS PARAMETERS

(Direct Variables)

Comparison	Sample Size	Correlation Coefficient	Regression Coefficients b	a	Scatter (km)
OBS/TELE	150	0.684	0.729	5.621	5.710
OBS/TRANS	150	0.238	0.069	16.579	7.608
OBS/NEPH	150	0.411	0.245	11.957	7.140
OBS/AVE NEPH	141	0.412	0.335	10.699	7.235
OBS/APVIS	150	0.606	0.323	10.916	6.232

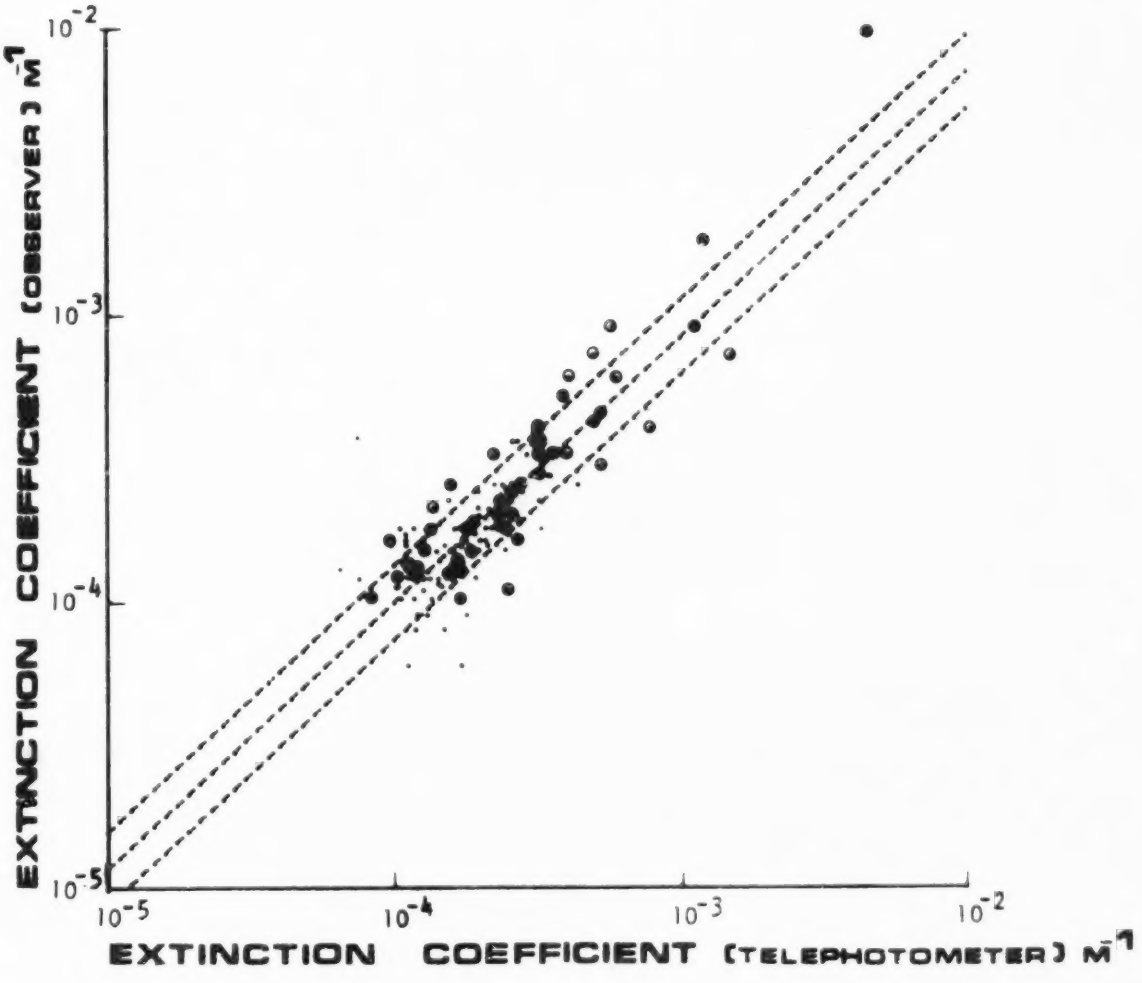

Figure 11: Scattergram of the observer and telephotometer derived extinction coefficients.

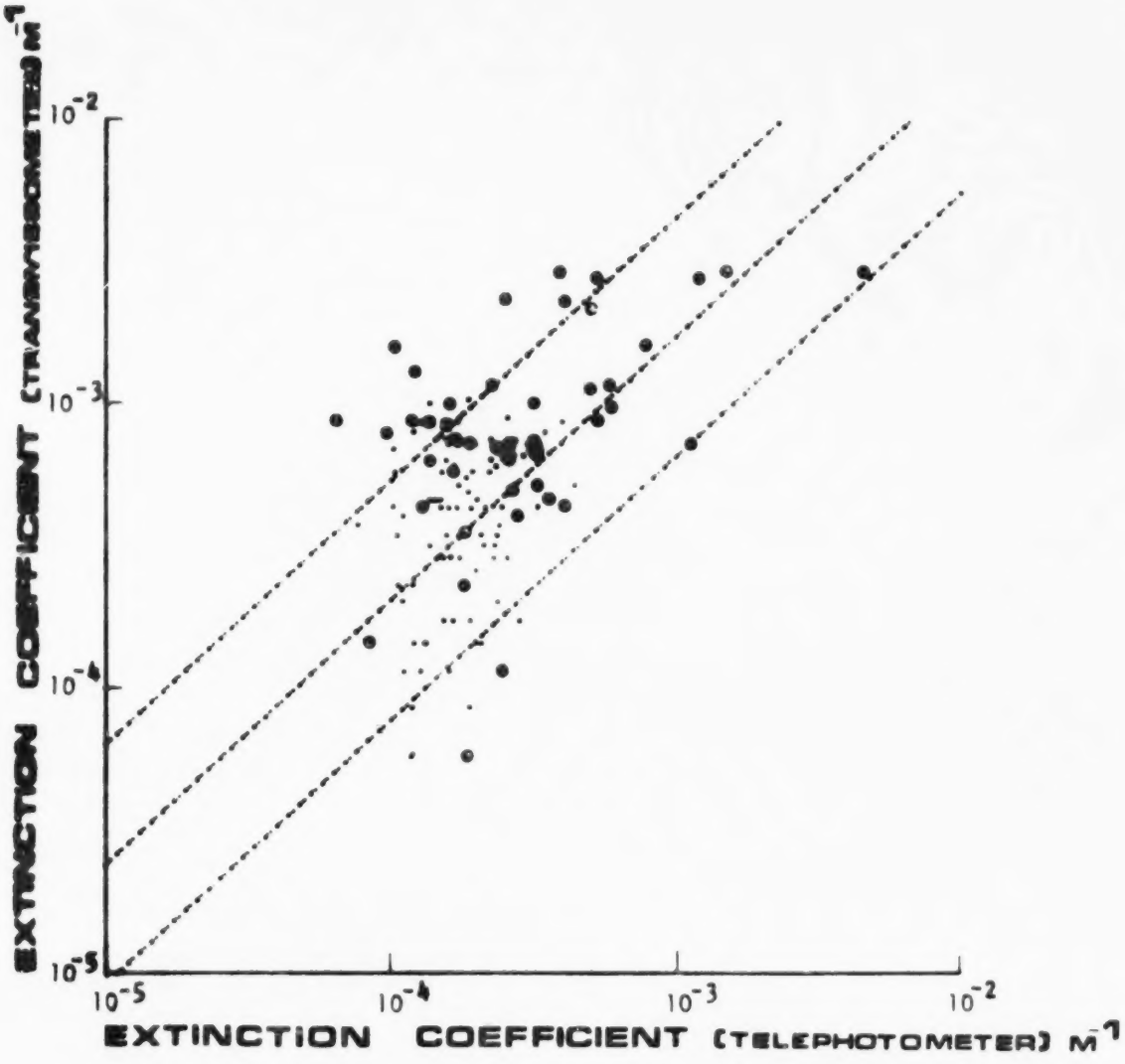

Figure 12: Scattergram of the transmissometer and telephotometer derived extinction coefficients

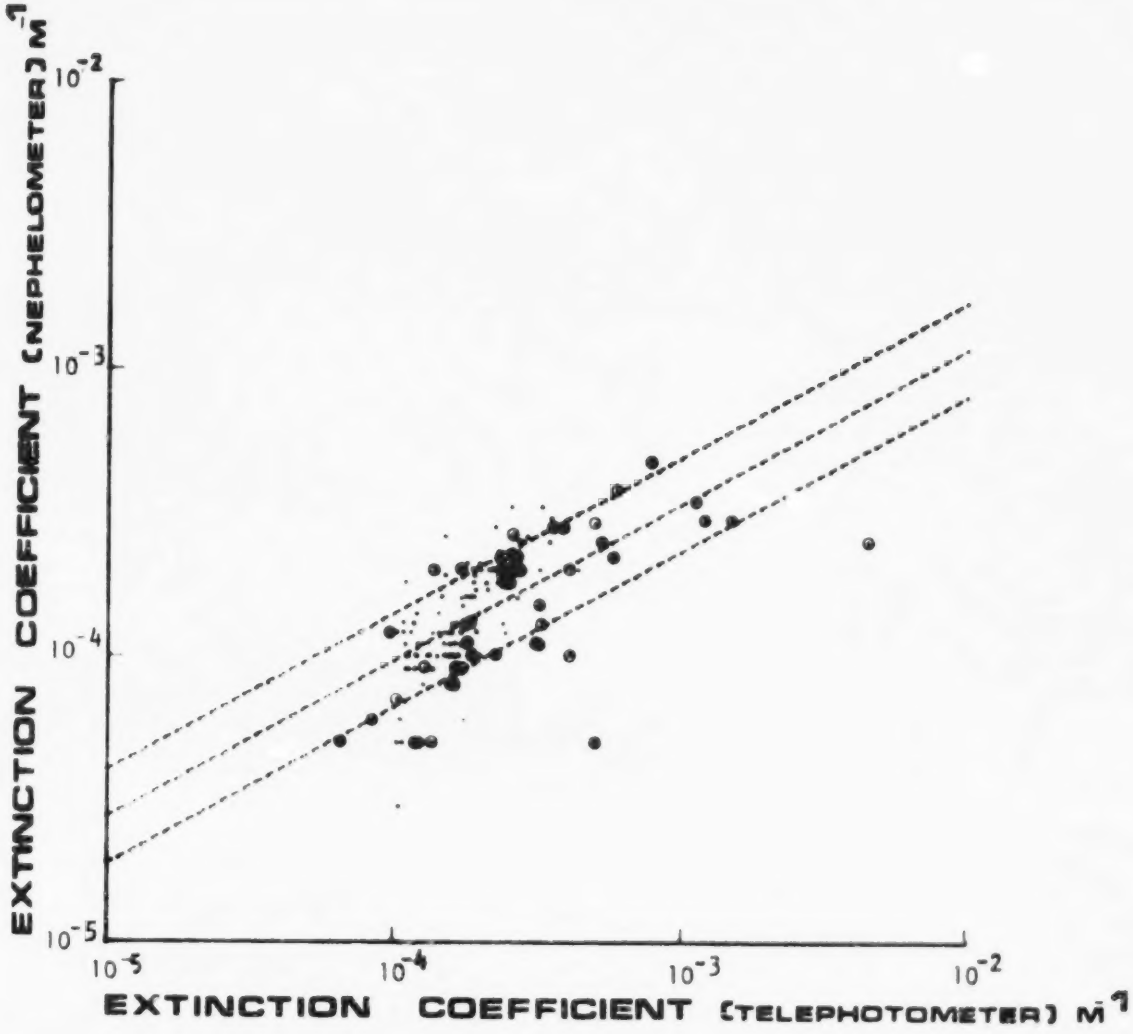

Figure 13: Scattergram of the nephelometer and telephotometer derived extinction coefficients.

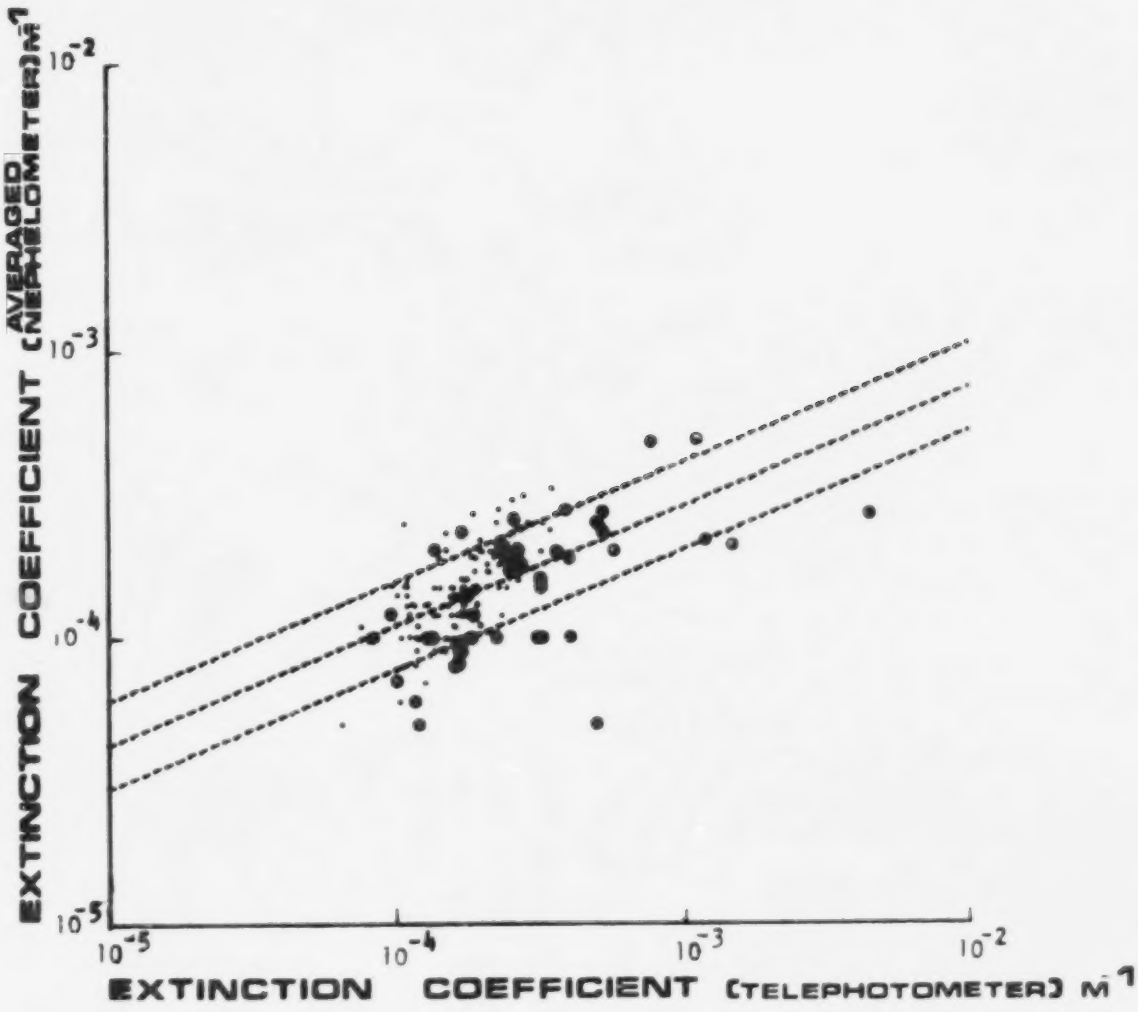

Figure 14: Scattergram of the averaged nephelometer and telephotometer derived extinction coefficients

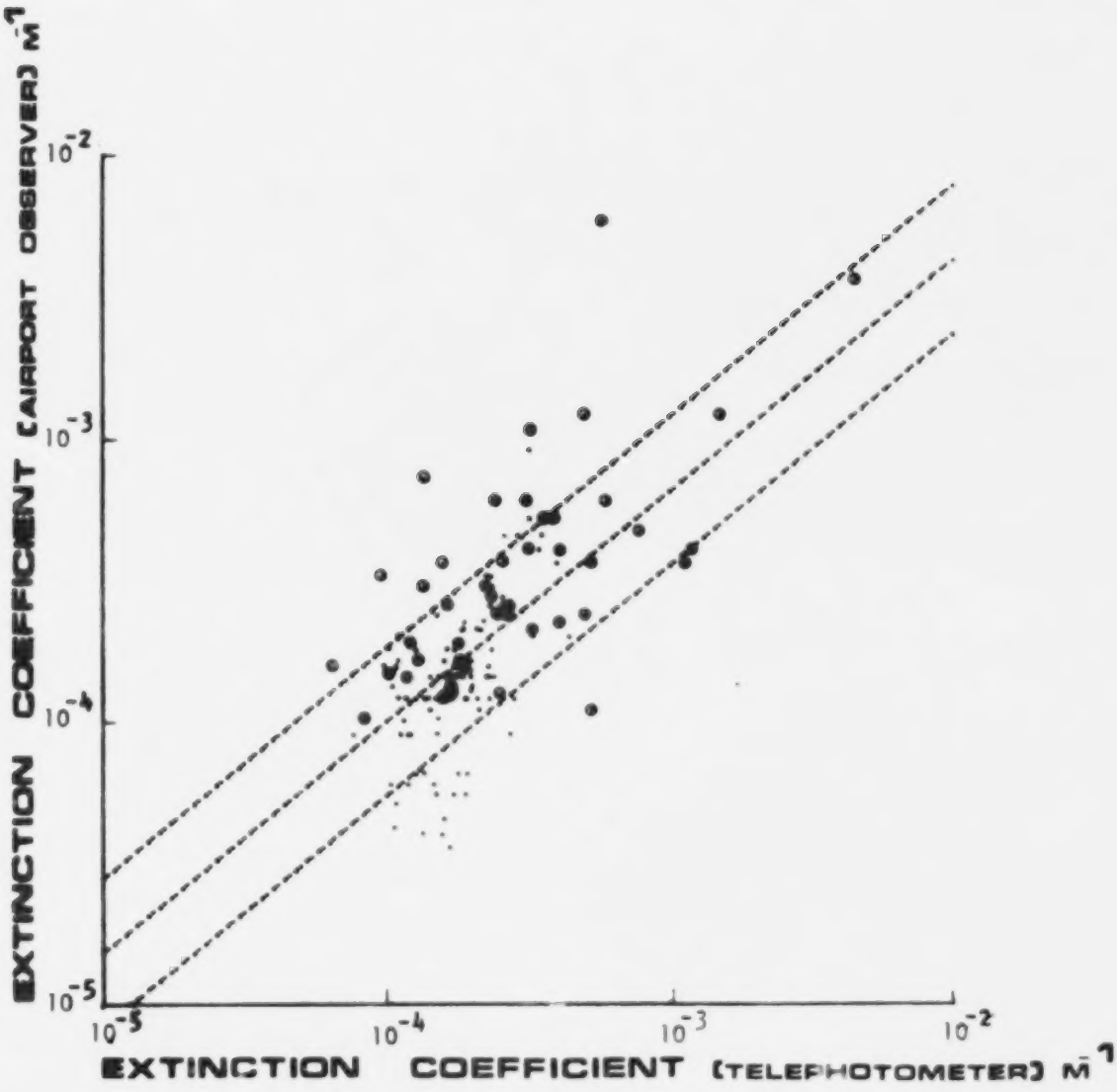

Figure 15: Scattergram of the airport observer and telephotometer derived extinction coefficients.

TABLE 5

SUMMARY OF REGRESSION ANALYSIS PARAMETERS

(Log-Log Variables)

Comparison	Sample Size	Correlation Coefficient	Regression Coefficients b	a	Scatter
OBS/TELE	150	0.874	0.924	-0.308	0.129
TRANS/TELE	150	0.485	0.925	0.009	0.420
NEPH/TELE	150	0.643	0.544	-1.842	0.163
AVE NEPH/TELE	141	0.568	0.414	2.302	0.152
APVIS/TELE	150	0.633	0.814	-0.745	0.262

comparison the relationship 2.9/V has been applied to the observer measurements. Results of these comparisons are presented in Table 6. Aside from the magnitude of the numbers, the most significant facts are that d is essentially constant with relative humidity for the observer-telephotometer comparison, exhibits a decreasing trend for the airport observer and shows increasing trends for all instruments. The conclusion here is that all instruments except the telephotometer respond to relative humidity effects.

COMPARISONS WITH PREVIOUS STUDIES

Previous studies involving the comparison of meteorological range derived from light scattering coefficients and human observer estimates of visibility have generally resulted in higher reported correlations. A comparison of reported correlations is given in Table 7 along with sample sizes and pertinent footnotings. The present results and those of Horvath and Noll *(1969)* are given for the relative humidity range of 0-65 percent while those of Samuels, Twiss and Wong *(1973)* are for relative humidities of 0-70 percent. It is to be noted that the NETL data yielded significantly lower correlations than reported by the other cited investigators. However, one-hour time averaging of the NETL nephelometer data yielded an increase in the correlation coefficient comparable to that obtained by Samuels, Twiss and Wong for eight hour averaging for both b_{scat} and observer estimates. Likely explanations for the lower NETL correlations are to be found in 1) the use of all data acquired, i.e., no attempt to subjectively sort the data was made on the basis that such sorting would not be representative of a real routine program, 2) the location of this experiment at ground level in a confined river valley, 3) location in an area where significant inhomogeneties in the atmospheric particle loadings occur, and 4) the use in previous studies of long-term average data (up to 8 hours), the data "smoothing" effects attendant to such averaging tending inevitably to produce higher correlations. The valley location dictated the use of slant paths for the telephotometer and transmissometer and precluded obtaining observer estimates of visibility in four quadrants except under low visibility conditions. Boundary layer meteorology and proximity to the Green River undoubtedly influenced the outcome of this experiment. In view of the consistency of the local observer-telephotometer results, the siting of the experiment (geographical location) is implicated in the results obtained for all other methods.

DISCUSSION OF INSTRUMENT PERFORMANCE

TELEPHOTOMETER

The telephotometer used during the tests proved to be a reliable instrument, easily portable and simple to use and to calibrate. The main difficulty with the instrument *per se* was that the angular field-of-view of the collecting optics was found to be larger than stated in the manufacturer's specification. This required the use of larger targets for target brightness measurements than was originally anticipated. For baselines much over one mile, in fact, the target size required for this instrument makes specially constructed targets largely impractical.

This latter point is, however, largely academic, because the advantage gained in optimally constructed special targets (i.e., "perfectly black" targets) viewed over relatively short (as compared to visual range) target baselines is rapidly lost in comparison with the advantage gained in using "gray" (natural) targets for viewing over optimal *baseline* lengths. Reasonable care in selecting such targets, with due consideration given to "correcting" the basic contrast data for the effects of intrinsic target brightness (Section VI), will assure good, reliable and repeatable data on which visibility estimates may be based.

TABLE 6

RMS FRACTIONAL DEVIATIONS:
TELEPHOTOMETER VERSUS ALTERNATE SYSTEMS

RH Range (Percent)	Visibility Method				
	OBS	APVIS	NEPH	AVE. NEPH	TRANS
0-65	0.908	0.924	0.277	0.240	1.974
0-80	0.906	0.915	0.284	0.291	2.297
0-90	0.904	0.907	0.309	0.310	2.795
0-100	0.902	0.898	0.365	0.371	3.104

TABLE 7

COMPARATIVE SUMMARY OF EXPERIMENTAL STUDIES

(Correlation Coefficients)

	0-65% RH		0-70% RH		
	b_{scat} NETL (a)	b_{scat} H & N (b)	b_{scat} S,T & W(La) (c)	b_{scat} S, T & W (oak)	b_{scat} S, T & W (sac)
OBS	(d) (-.596) -.537	(f) -0.90	(e) (-0.922) -0.873	(e) (-0.919) -0.837	(e) (-0.958) -0.913
Data Points	55	67	601	356	60

(a) This report

(b) Horvath and Noll, Reference 1

(c) Samuels, Twiss and Wong, Reference 9

(d) One-Hour Average b_{scat}

(e) Eight-Hour Average b_{scat} and Observer

(f) Average of two sets of observations to which wavelength corrections were applied.

A serious drawback of the evaluated telephotometer is that it requires manual operation, and cannot be readily adpated to automated use. This is not to say it could not be so adapted, but it would require some rather fundamental design changes in the basic instrument system. The singular disadvantage of the system is that it cannot be readily adapted for nighttime use, i.e., for the measurement of nighttime visibility.

TRANSMISSOMETER

Again, the transmissometer used proved to be a reliable instrument, operating continuously over a 24-hour duty cycle. The initial instrument set-up and calibration was simple to perform.

The main disadvantage of the transmissometer as a visibility monitor is that it is "locked" to a fixed baseline measurement. Consequently, estimates of extreme visibilities (either very long or very short) are subject to large interpretation errors. The flexibility in choosing targets to optimize baseline length according to prevailing visibility afforded by the telephotometer, is not available to the transmissometer. The instrument is thus best suited for use in a "yes/no" mode of operation, i.e., as a continuous monitor to tell when atmospheric conditions result in visibilities of a specified value. The baseline can then be tailored specifically to that visual range estimate.

The transmissometer also proved sensitive to refraction effects. Initially, gross beam bending in response to the optical refractive index gradient caused an effective mislignment of the transceiver/retroflector system. The addition of a scanning transceiver mount to maximize the received signal intensity effectively eliminated this effect. However, beam defocusing effects due to beam spreading by turbulence in the refractive index field continued to impose an effective additional attenuation on the received signal, especially during hot, bright days. This effect could be eliminated by a simple design change in the retroreflector (i. e., a large array of small retroreflectors as opposed to a small array of large reflectors).

Because transmission measurements relate to the total extinction coefficient, absorption attenuation by aerosol particles and water vapor could result in some error in the estimate of *daytime* visibility on excessively humid days. However, the effect would be small, and, in fact, for *nighttime* visibility estimates, the effect is to be desired.

NEPHELOMETER

The nephelometer, too, proved to be a reliable instrument, readily set-up and put into operation, and easily portable. Calibration of the instrument involved the most complicated procedure of any of the instruments used during the tests, but the calibration runs did produce consistent and repeatable results.

In operating the instrument, however, care must be taken to assure that the humidity of the sampled air is maintained at the ambient level. The size distribution of the hygroscopic particles of the atmospheric aerosol is sensitive to relatively small changes in humidity, and any alteration of that distribution leads to errors in the estimate of visibility from the volume scattering coefficient measurements.

Because aerosol particle absorption also contributes to the total extinction measured by the nephelometer *, it is best used for estimates of the nighttime visual range. Converse to the case of the transmissometer, however, its use for nighttime visibility estimates will result in erroneous data if water vapor absorption figures prominently in the total extinction.

The singular disadvantage of the nephelometer for visibility estimates is that it performs a "point" measurement, whereas visibility is a function of an "integrated" atmospheric state. Consequently, the response of the nephelometer to horizontal advection of spatial inhomogeneities in the atmospheric particle loading can be excessive. This effect was after noted in a comparison of continuous recordings of transmissometer and nephelometer data. Given homogeneous atmospheric conditions, the two sets of data "tracked" well; at other times, there was no apparent correlation between them. *Time-averaging of nephelometer data will serve as some sort of spatial average of the inhomogeneous atmosphere, but only in an effective azimuth corresponding to the wind direction;* i.e., a time-averaged nephelometer trace would correspond to a transmissometer trace obtained with a baseline oriented in the direction of the mean wind, with the averaging interval defined by T=(mean wind speed)/baseline length).

INTERPRETATION OF FIELD DATA

GENERAL

Within the limitations of the field experiment, the implications of an error analysis (Appendix A) have been by and large born out by the field test results. The limited "sample sizes" constituting the field data preclude a precise qualitative verification of those implications, but some of the qualitative comparisons between theory and experiments are presented below.

First, by far the best correlation between observer and instrument-derived visibility estimates were obtained with the telephotometer (Table 3). This is due for the most part to the flexibility allowed by the telephotometer in making the required measurements. Not only was the natural target baseline selection optimized, but the acquired data were obtained over all quadrants, and the results averaged to define the visibility for a given observation run. This latter process minimized the effect of inhomogeneities in the spatial distribution of the aerosol loading in biasing the visibility estimates to excessive values in a fixed azimuth.

*Absorption previously assumed to be negligible in the integrating nephelometer is presently being investigated.

VISUAL RANGE DEPENDENCE

In developing the data shown in Table 4, sample sizes in each sub-category of the total data collected were too small to yield statistically significant results. Nevertheless, the data so developed do tend to substantiate in at least a qualitative manner the implications of Figures 16 and 17. That is, best correlation is to be found between the logarithms of the visual ranges noted by the observer and as derived from data obtained with both the transmissometer and telephotometer for the lowest values of prevailing visibility (Table 3a). Baseline transmittances for both the transmissometer and for the telephotometer in relation to the special targets were in this case of the order 0.4, close to the optimum value. With progressively greater prevailing visibilities, the correlations between observer and instrument estimates of visual ranges deteriorated (Tables 3b, 3c, 3d) as baseline transmittances progressively increased to values of the order 0.8. Any error in the instrument readings would in this latter case carry more than three times the impact on the visual range estimate (Figures 16 and 17) than for the case of the lowest prevailing visibility.

Compounding the effect just discussed is the fact that at extreme visual ranges (Table 3d) the reliability of the observer estimate of visual range can itself be questioned. The point is somewhat moot, however, because it is the low visibilities that are of concern relative to questions of air quality.

As might be expected, there is no clear-cut, systematic variation in the nephelometer/observer visual range correlation through the various prevailing categories. However, it is perhaps worth mentioning that the highest correlation in the instrument-derived data is to be found between the log V data as determined by the nephelometer and telephotometer when the prevailing visibility was greater than 24 km. This result is consistent with Figure 18. That is, the clearer the air, the smaller are the particles of the atmospheric aerosol likely to be, and the larger will be the size parameter of the Junge distribution, equation (A52), Appendix A, that characterizes the particle size distribution. The less, therefore, will be the impact of angular truncation errors on nephelometer-derived visibility estimates.

Finally, during field operations the lowest visibilities recorded (0-8 km) were frequently associated with relatively shallow layers of ground fog advected off the Green River. These layers tended to be rather patchy in nature, and the nephelometer data therefore tended to show wide excursions during ground fog occurances in response to horizontal advection of the spatial variations in aerosol particle loadings. This is the origin of the fact that whereas the best correlations between transmissometer and telephotometer versus observer visibility data (log) were obtained during low visibility conditions (Table 3a), and in accordance with Figures 16 and 17, the nephelometer data showed essentially the poorest correlation. The correlation between nephelometer and telephotometer data was also lowest in the 0-8 km prevailing visibility category. This behavior illustrates the major disadvantage of the nephelometer for visibility estimates, viz., the use of "point" measurements to characterize an essentially "integrated" atmospheric condition.

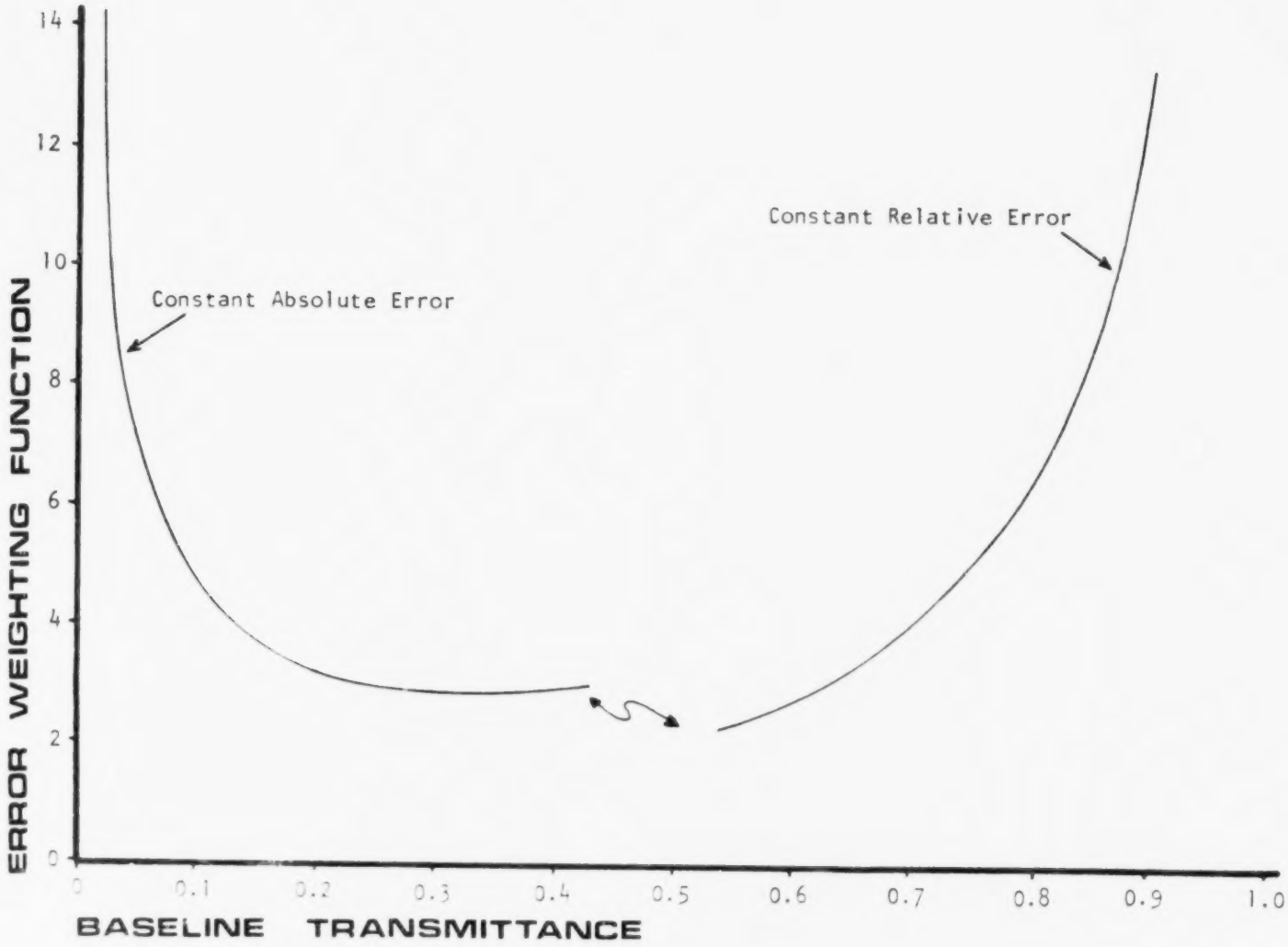

Figure 16: Composite error weighting function - Transmissometer.

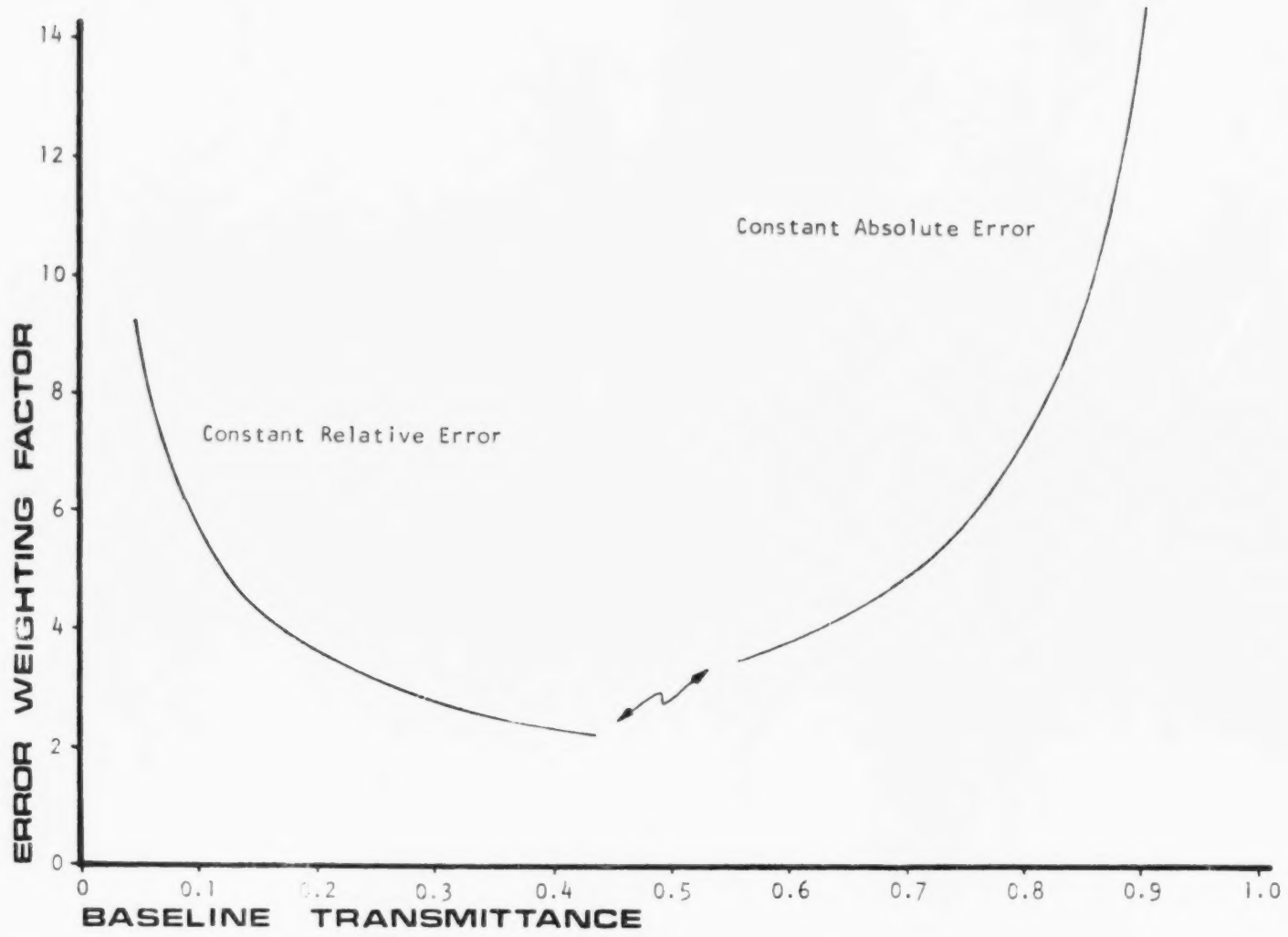

Figure 17: Composite error weighting function - Telephotometer.

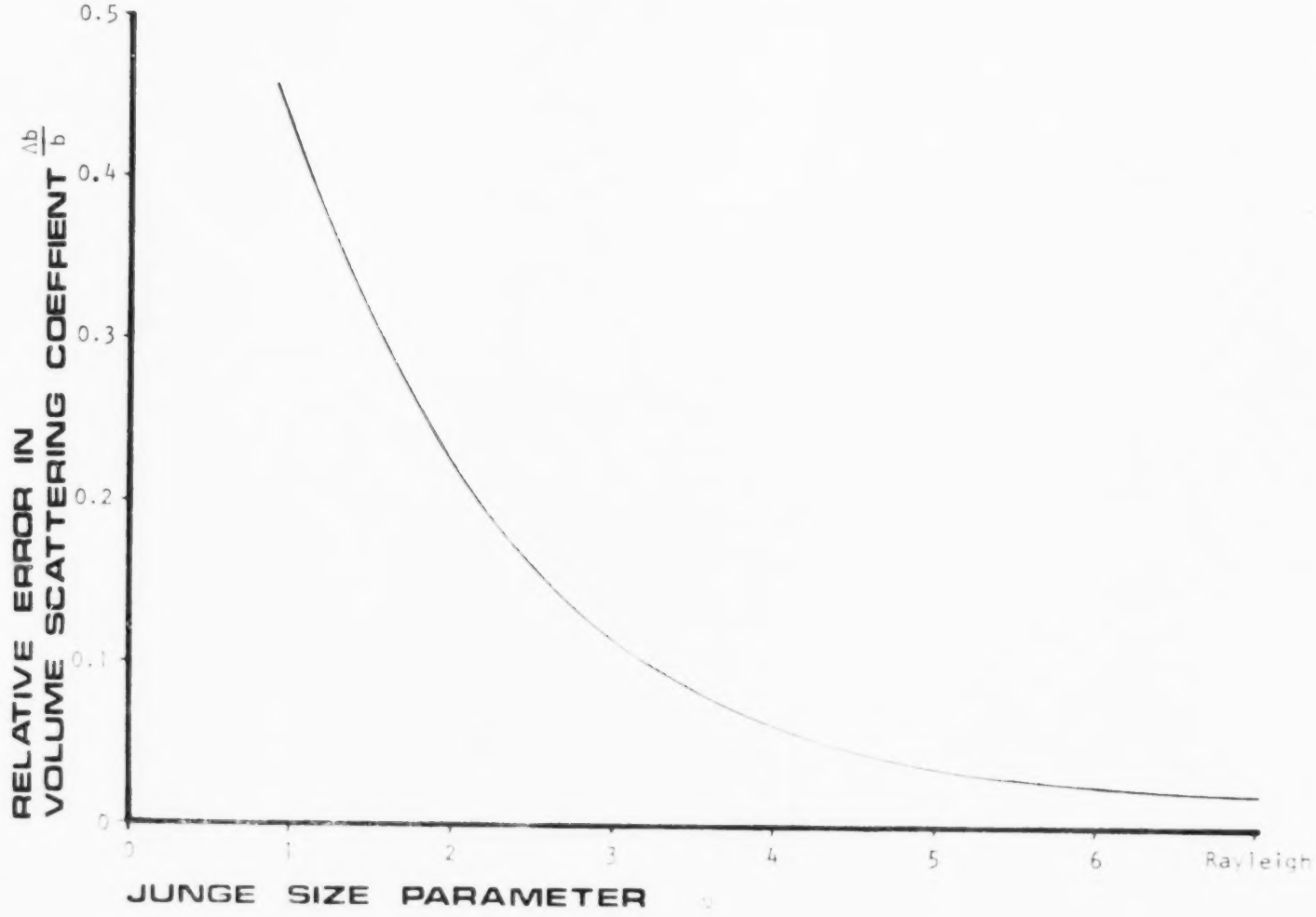

Figure 16: Relative error in the volume scattering coefficient.

RELATIVE HUMIDITY EFFECTS

The total extinction is the sum of scattering and absoprtion attenuation. It is a consequence of Duntley's law, however, that the contrast of perfectly black objects viewed against the horizon sky is never increased by absoprtion. Thus, from the standpoint of the definition of *daylight* visual range, it is only the scattering attenuation component of the total extinction that determines the daylight visual range (*Middleton, 1952*).

Of the three instruments used during the field tests, only the telephotometer functions in response to scattering attenuation *per se*, albeit implicitly through the direct measurement of contrast. Both the nephelometer and transmissometer measurements reflect the effects of absorption by aerosol particles of complex dielectric constant. The effect may be compounded in the transmissometer measurement by water vapor continuous absorption in the vicinity of 0.6328 μm, the wavelength of the He-Ne laser source. If so, the interpretation of nephelometer- and transmissometer-derived *extinction* data would yield an underestimate of the true visibility, with worst results obtained with the transmissometer under excessively humid conditions. This effect may be the origin of the increasing rms fractional deviation relative to the telephotometer with increasing relative humidity (Table 6).

It should be remarked, however, the above argument would hold only in regard to the estimate of *daytime* visibility. Nighttime visibility is defined in reference to the apparent brightness of a standard light source. The governing law in this case is essentially Allard's law, and therefore it is the total *extinction* that determines the apparent brightness. In other words, the fact that the nephelometer and transmissometer respond to total particle extinction would work to advantage in the estimate of nighttime visibility.

Before leaving the discussion of humidity effects, the importance of the data shown in Figure 4 must be reemphasized. That is, in using the nephelometer for obtaining visibility estimates, it must be assured that the humidity of the sampled air is maintained at the ambient level, in order that the size distribution of hydroscopic particles of the atmospheric aerosol is not altered during the sampling process. Any such alteration would result in erroneous volume scattering coefficient measurements (*Waggoner, et al., 1973*), and therefore erroneous visibility estimates.

SECTION VI

REFERENCES

1. Horvath, H. and K. E. Noll. "The Relationship Between Atmospheric Light Scattering Coefficient and Visibility." *Atmospheric Environment*. 3: 543-552. 1969.

2. Kerker, M. *The Scattering of Light and Other Electromagnetic Radiation*. Academic Press, New York. 1969.

3. Middleton, W. E. K. *Vision Through the Atmosphere*. University of Toronto Press. 1952. 250 pp.

4. Duntley, S. Q. "The Optical Properties of Diffusing Materials." *JOSA* 38: 237-249. 1948.

5. Blackwell, H. R. "Report of Progress of the Roscommon Visibility Tests. June 1947 - December 1948. Paper read to the Aviation Lighting Committee of the I.E.S. at Washington, D.C. April 21.

6. "An Analysis of Visual Range." Federal Aviation Agency: Report No. RD-66-100, AD No. 658-537. 1966.

7. Middleton, W. E. K. "The Measurement of Visibility at Night. Part II." *Trans Royal Soc. Canada*, Sec. III 26: 25-33. 1932.

8. Nie, Norman, Dale H. Bent and C. Hodlai Hull. *Statistical Package for the Social Sciences*, McGraw-Hill Book Company, New York. 1970. 341 pp.

9. Samuels, Harris J., SuzAnne Twiss, and Evan W. Wong, "Visibility, Light Scattering and Mass Concentration of Particulate Matter", *Report of the California Tri-City Aerosol Sampling Project*, State of California, Air Resources Board. 1973.

10. Waggoner, A. P., N. C. Ahlquist, and R. J. Charlson. "Measurement of the Aerosol Total Scatter-backscatter Ratio." *Appl. Op.*, to be published.

SECTION VII

APPENDICES

A. Error Analysis

B. Observations

C. 24-Hour Suspended Particulate Concentrations

D. Scattering Coefficients

APPENDIX A

ERROR ANALYSIS

The following error analysis is offered as the basis for the interpretation of the results given in Section V.

With either the transmissometer or the telephotometer, the quantity measured for the estimate of visibility is, or can be converted to, the transmittance, τ, of a thickness, R, of the atmosphere. Restating the Bouguer-Lambert law with the extinction coefficient expressed in terms of the daylight visibility.

$$\ln \tau = - \frac{2.9R}{V} . \qquad (A1)$$

The differential of equation (A1) may be written in terms of finite increments as,

$$\frac{\Delta\tau}{\tau} = \frac{2.9R}{V} \frac{\Delta V}{V} , \qquad (A2)$$

and therefore,

$$\frac{\Delta V}{V} = - \frac{1}{\ln \tau} \frac{\Delta \tau}{\tau} . \qquad (A3)$$

Equation (A3) thus indicates that the relative error in the visibility estimates is given by the relative error in the transmittance measurement, weighted by the reciprocal of the (natural) logarithm of the transmittance over the instrument "baseline" R. Squaring, averaging and taking the square root of both sides of equation (A3) yields for the rms error equation,

$$\left\langle \left(\frac{\Delta V}{V} \right)^2 \right\rangle^{1/2} = \frac{1}{|\ln \tau|} \left\langle \left(\frac{\Delta \tau}{\tau} \right)^2 \right\rangle^{1/2} , \qquad (A4)$$

or, changing symbolism,

$$\epsilon_V = \frac{1}{|\xi n_T|}\,\epsilon_T \,, \tag{A5}$$

where the epsilons denote the rms errors of the variables indicated by the subscripts.

For the nephelometer, the quantity measured for the estimate of visibility is the volume extinction coefficient, b. The relationship between b and the daylight visibility is (Section IV),

$$b = \frac{2.92}{V} \tag{A6}$$

Differentiating logarithmically,

$$\frac{\Delta b}{b} = -\frac{\Delta V}{V} \tag{A7}$$

Again squaring, averaging, and taking the square root of both sides of equation (A7), there results, using the rotation introduced previously,

$$\epsilon_V = \epsilon_b \tag{A8}$$

In this case there is thus a simple one-to-one correspondence between the measurement error and the visibility estimate. The quantitative analysis of the impact of transmissometer, telephotometer, and nephelometer measurement errors on the visibility estimate follows.

TRANSMISSOMETER

The measurement performed with the transmissometer is of the ratio of the received (after propagation over the transmissometer baseline) to the intrinsic source intensity,

$$\tau = \frac{I_R}{I_0} \tag{A9}$$

or,

$$\ln \tau = \ln I_R - \ln I_o \quad . \tag{A10}$$

The differential form of equation (A10) relates the relative transmittance error to the relative errors in the intensity measurements; i.e.,

$$\frac{\Delta\tau}{t} = \frac{\Delta I_R}{I_R} - \frac{\Delta I_o}{I_o} \tag{A11}$$

Assuming uncorrelated measurement errors, the square root of equation (A11) squared and averaged may be stated,

$$\epsilon_\tau = \left[\left\langle \left(\frac{\Delta I_R}{I_R} \right)^2 \right\rangle + \left\langle \left(\frac{\Delta I_o}{I_o} \right)^2 \right\rangle \right]^{1/2} \quad . \tag{A12}$$

Two possibilities must now be considered in regard to the behavior of the system measurement errors, viz., (1) constant *relative* intensity errors (i.e., the mean square *ratios* $\Delta I/I$ constant, implying absolute errors -- mean square increment values -- proportional to the intensity levels), and (2) constant *absolute* errors (i.e., the magnitudes of $\langle (\Delta I_R)^2 \rangle$ and $\langle (\Delta I_o)^2 \rangle$ independent of those of I_R and I_o).

CONSTANT RELATIVE INTENSITY ERRORS

If the transmissometer performs such that the relative measurement errors are constant, equation (A12) may be stated,

$$\epsilon_\tau = \left[\epsilon^2_{I_R} + \epsilon^2_{I_o} \right]^{1/2} = \epsilon'_I \quad , \tag{A13}$$

say, where ϵ'_I denotes the square root of the sum of the mean square errors in the intensity measurements. Substituting equation (A13) into equation (A5),

$$\epsilon_v = \frac{1}{|\ln \tau|} \epsilon'_I = W(\tau) \quad , \tag{A14}$$

say, where τ is the baseline transmittance. Thus,

$$\varepsilon_V = \frac{V}{2.9R}\,\varepsilon_I' = 0.34\,\frac{V}{R}\,\varepsilon_I' \qquad \text{(A15)}$$

For this case then, equation (A15) indicates that the rms error in the visibility estimate is given by the rms error in the intensity measurements, *weighted by the ratio of the visual range to the transmissometer baseline length.* Equation (A15) thus allows specification of the minimum baseline required for a specified accuracy in the visual range estimate. For example, without loss of generality, equation (A12) may be stated for the case $\varepsilon_{I_R} = \varepsilon_{I_o} = \varepsilon_I$,

$$\frac{V}{R} = \frac{2.9}{\sqrt{2}}\,\frac{\varepsilon_V}{\varepsilon_I} \qquad \text{(A16)}$$

Suppose then, a 10 percent accuracy is desired in the visibility measurement, and say the intensity measurements can be made to an accuracy of 2 percent. The maximum visibility-to-baseline ratio which would allow the stated accuracy in the visibility estimate would then be,

$$\frac{V}{R} = \frac{2.9}{\sqrt{2}}\,\frac{0.10}{0.02} = 10.3.$$

In an atmosphere characterized by a 10 mile visual range, a nearly one mile instrument baseline would be required to effect the visual range measurement to 10 ± 1 mile.

CONSTANT ABSOLUTE INTENSITY ERRORS

For the case of constant absolute intensity errors, consider that equation (A12) may be written,

$$\varepsilon_\tau = \left[\frac{1}{I_R^2}\left\langle(\Delta I_R)^2\right\rangle + \frac{1}{I_o^2}\left\langle(\Delta I_o)^2\right\rangle\right]^{1/2}, \qquad \text{(A17)}$$

or, recognizing that $I_R = I_o\tau$ [equation (A6)],

$$\varepsilon_\tau = \frac{1}{I_o\tau}\left[\left\langle(\Delta I_R)^2\right\rangle + \tau^2\left\langle(\Delta I_o)^2\right\rangle\right]^{1/2}. \qquad \text{(A18)}$$

Without loss of generality, consider the case $\left\langle (\Delta I_R)^2 \right\rangle = \left\langle (\Delta I_o)^2 \right\rangle = \delta^2$. Equation (A18) may then be written

$$\varepsilon_\tau = \frac{\delta}{I_o} \frac{(1+\tau^2)^{1/2}}{\tau} \quad , \tag{A19}$$

and therefore, substituting equation (A19) into equation (A5),

$$\varepsilon_V = \frac{\delta}{I_o} \left[\frac{(1+\tau^2)^{1/2}}{\tau \ell n \tau} \right] \qquad \text{a)}$$

$$= \frac{\delta}{I_o} \; W(\tau) \; , \qquad \text{b)} \tag{A20}$$

say, the ratio δ/I_o on the right hand sides of equations (A11) defines, in effect, the magnitude of the intensity measurement error in terms of a percentage of the intrinsic source intensity.

The measurement error weighting factor, $W(\tau)$, is more complex in this than in the previous case. Differentiating equation (A11a) with respect to τ,

$$\frac{d\varepsilon_V}{d\tau} = \frac{\delta}{I_o} \frac{1}{\tau \ell n \tau} \left[\frac{\tau}{(1+\tau^2)^{1/2}} - \frac{(1+\tau^2)^{1/2}(1+\ell n \tau)}{\tau \ell n \tau} \right]; \tag{A21}$$

setting this result equal to zero and rearranging terms yields

$$\ell n \; \tau = - \; (1 + \tau^2). \tag{A22}$$

The root of the above transcendental equation indicates that the minimum error in the visibility estimate occurs when the transmittance of the atmosphere over the instrument baseline attains the value about $\tau = 0.33$. The error weighting factor does exhibit, however, a rather broad "minimum." This is indicated by the plot of $W(\tau)$ versus τ as defined here [and

also that defined by equality (A14)] shown in Figure A-1. For example, assuming once more the 2 percent measurement error (i.e., $\delta/1 = 0.02$) and a desired accuracy of 10 percent in the visibility estimate, Figure 12 indicates $W_{trans}(\tau) \leq 5$ for transmittances in the range about $0.08 \leq \tau \leq 0.71$. Over a one mile instrument baseline then, visibility could be specified to the desired 10 percent accuracy in the range of about $1.1 \leq V \leq 8.8$ miles.

TELEPHOTOMETER

From Duntley's law of contrast reduction

$$\tau = \frac{(B_R - B_h)}{(B_o - B_h)} ; \tag{A23}$$

or,

$$\ln \tau = \ln (B_R - B_h) - \ln (B_o - B_h) \tag{A24}$$

where, recapitulating, B_R is the apparent brightness of a remote target of intrinsic brightness B_o viewed over a telephotometer baseline R, and B_h is the brightness of the adjacent horizon sky. The ideal target is perfectly black, i.e., $B_o = 0$. The brightnesses B_R and B_h are the parameters measured telephotometrically; for non-black targets B_o is dependent on the physical characteristics of the target, e.g., surface albedo.

Operating on equation (A24) as outlined in the previous section, rearranging terms and utilizing equation (A23),

$$\varepsilon_\tau = \frac{B_h}{(B_h - B_o)} \left\{ \left[\frac{(B_h - B_o)}{B_h} - \frac{1}{\tau} \right]^2 \left\langle \left(\frac{\Delta B_R}{B_R} \right)^2 \right\rangle + \frac{(1-\tau)^2}{\tau^2} \left\langle \left(\frac{\Delta B_h}{B_h} \right)^2 \right\rangle + \left(\frac{B_o}{B_h} \right)^2 \left\langle \left(\frac{\Delta B_o}{B_o} \right)^2 \right\rangle \right\}^{1/2} \tag{A25}$$

Inherent in the above statement is again the assumption of uncorrelated brightness measurement errors. To be considered now are the two cases mentioned previously, viz, constant relative rms errors, and constant absolute rms errors.

CONSTANT RELATIVE BRIGHTNESS ERRORS

Recognize that,

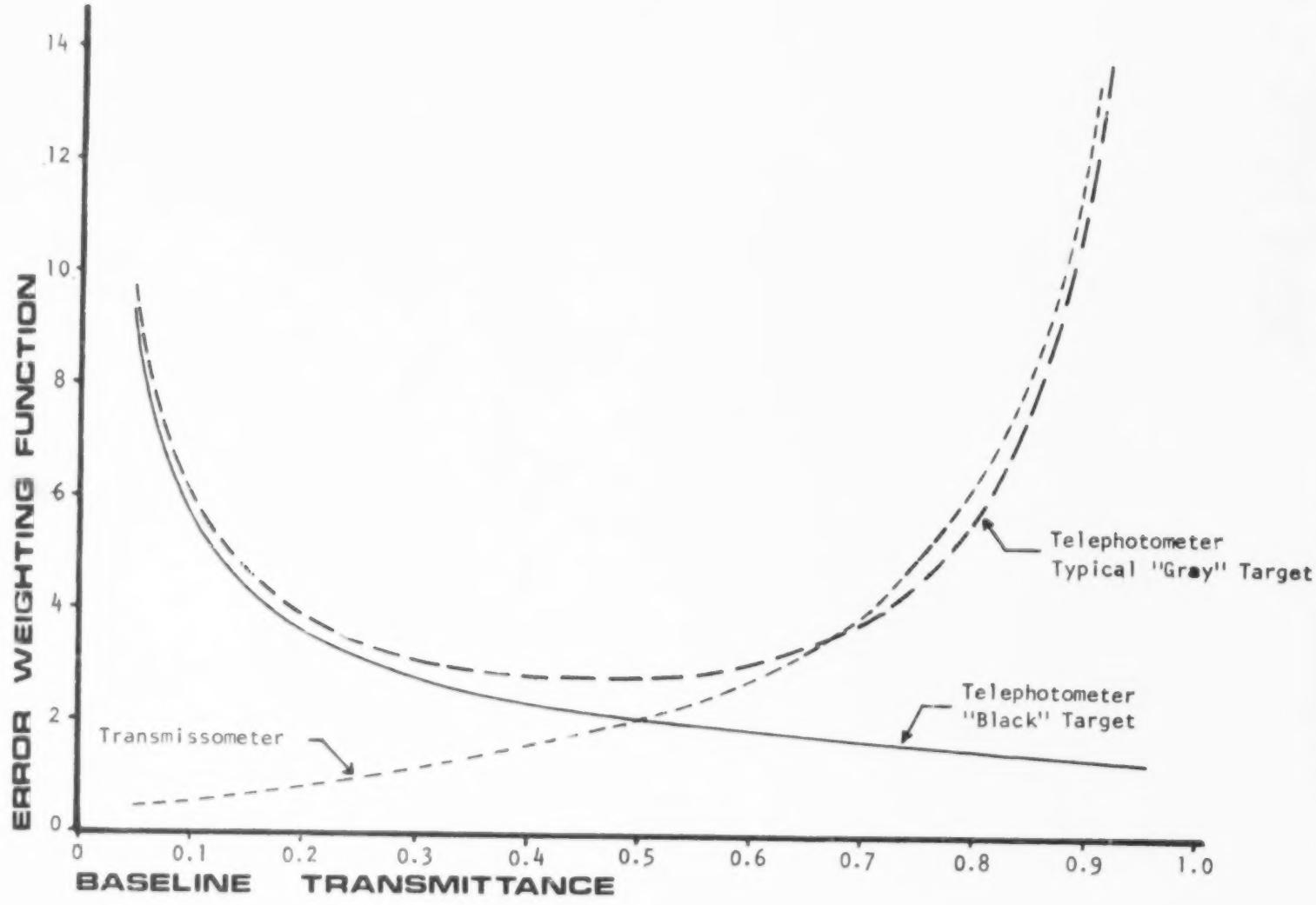

Figure A-1: Constant relative measurement errors.

$$\frac{B_h - B_o}{B_h} = |C_o| \tag{A26}$$

the magnitude of the intrinsic target contrast with equation (A26), equation (A25) may be stated for the case of constant relative brightness errors,

$$\varepsilon_\tau = \frac{1}{|C_o|}\left[\frac{(1 - |C_o|\,\tau)^2}{\tau^2}\,\varepsilon_{B_R}^2 + \frac{(1-\tau)^2}{\tau^2}\,\varepsilon_{B_h}^2 + (1 - |C_o|)^2\,\varepsilon_{B_o}^2\right]^{1/2} \tag{A27}$$

where the symbolism is as introduced previously.

Equation (A27) illustrates a much more complex dependence of the transmittance error on the measurement errors than does equation (A13). Two further cases must now be considered, viz., the case of the ideal "black" target, and the case of the "gray" target.

IDEAL BLACK TARGET

Note from equation (A26) that for an ideal black target (or at least when $B_h >> B_o$), $C_o = 1$ and equation (A27) reduces to,

$$\varepsilon_\tau = \frac{(1-\tau)}{\tau}\left[\varepsilon_{B_R}^2 + \varepsilon_{B_h}^2\right]^{1/2} \tag{A28}$$

Again without loss of generality consider,

$$\varepsilon_{B_R}^2 = \varepsilon_{B_h}^2 = \varepsilon_B^2 \tag{A29}$$

Now utilizing equations (A28 and A29) in equation (A5),

$$\varepsilon_V = \sqrt{2}\left[\frac{(1-\tau)}{\tau\,\ell n\tau}\right]\varepsilon_B \tag{A30}$$

The measurements error weighting factor (the coefficient of ε_B) dictates a dependence of the visibility estimate error on ε_B and on τ -- i.e., on the ratio V/R -- which is the direct opposite of the dependence cited for the transmissometer measurements; i.e., in this case, the greater the

transmittance over the telephotometer baseline, the *better* is the visibility estimate. The error weighting factor in equation (A30) with that in equation (A14) for $\varepsilon_i' = 2\,\varepsilon_i$, is plotted against transmittance in Figure A-2. Note that for relative measurement errors equal in magnitude, the transmissometer and the telephotometer yield equivalent accuracies in the visibility estimate for baseline transmittances $\tau = 0.5$. When $\tau > 0.5$, the telephotometer gives the better result; when $\tau > 0.5$, the reverse is true. It should be emphasized that this result holds (1) when the *relative* measurement errors are constant, and (2), when the telephotometer is used to view an ideal, black target.

"GRAY" TARGET

The intrinsic brightness of a "gray" object derives basically from that of its surroundings; i.e., light from diffusely reflecting surroundings is once more (diffusely) reflected by the object and redirected to the eye of the observer and perceived as the object brightness. The characterization of object brightness in terms of that of its surroundings is thus an extremely complex problem, depending as it does on the directional reflectances of both object and surroundings, and on the brightness distribution over the dome of the light-scattering sky. If, however, sky brightness is assumed to vary monotomically with the cosine of the zenith angle, and both the object and its surrounding are characterized as Lambertian reflectors of reflectances R and R', respectively, the intrinsic brightness of a gray object can be stated as [*Middleton, 1952*],

$$B_{go} = B_h \left[\frac{R}{2}(1+R') + \frac{nR}{3}\left(\frac{2}{\pi} + R'\right) \right], \qquad \text{(A31)}$$

where the subscript "go" on the left hand side denotes the intrinsic brightness of a "gray" object, and where n is a parameter incorporated in the specification of the brightness of an element of the sky at a specified zenith angle in terms of the horizon sky brightness; Middleton, [*1952*] suggests the value n = 2.

Taking the logarithmic differential of equation (A31) and rearranging terms,

$$\frac{\Delta B_{go}}{B_{go}} = \frac{\Delta B_h}{B_h} + \frac{B_h}{B_{go}} \left\{ \frac{7}{6} RR' \frac{\Delta R'}{R'} + \left[\frac{(3\pi+8)R + 7\pi RR'}{6\pi} \right] \frac{\Delta R}{R} \right\} \qquad \text{(A32)}$$

A representative value for both R and R' may be taken as 0.1 (*Stewart and Hopfield, 1965*; *Smithsonian Tables, 1966*), applying to "dark" buildings and vegetated foregrounds. Utilizing these values in equation (A32) and with the definition given in equation (A26), the mean square error form of equation (A32) may be stated, again assuming uncorrelated errors,

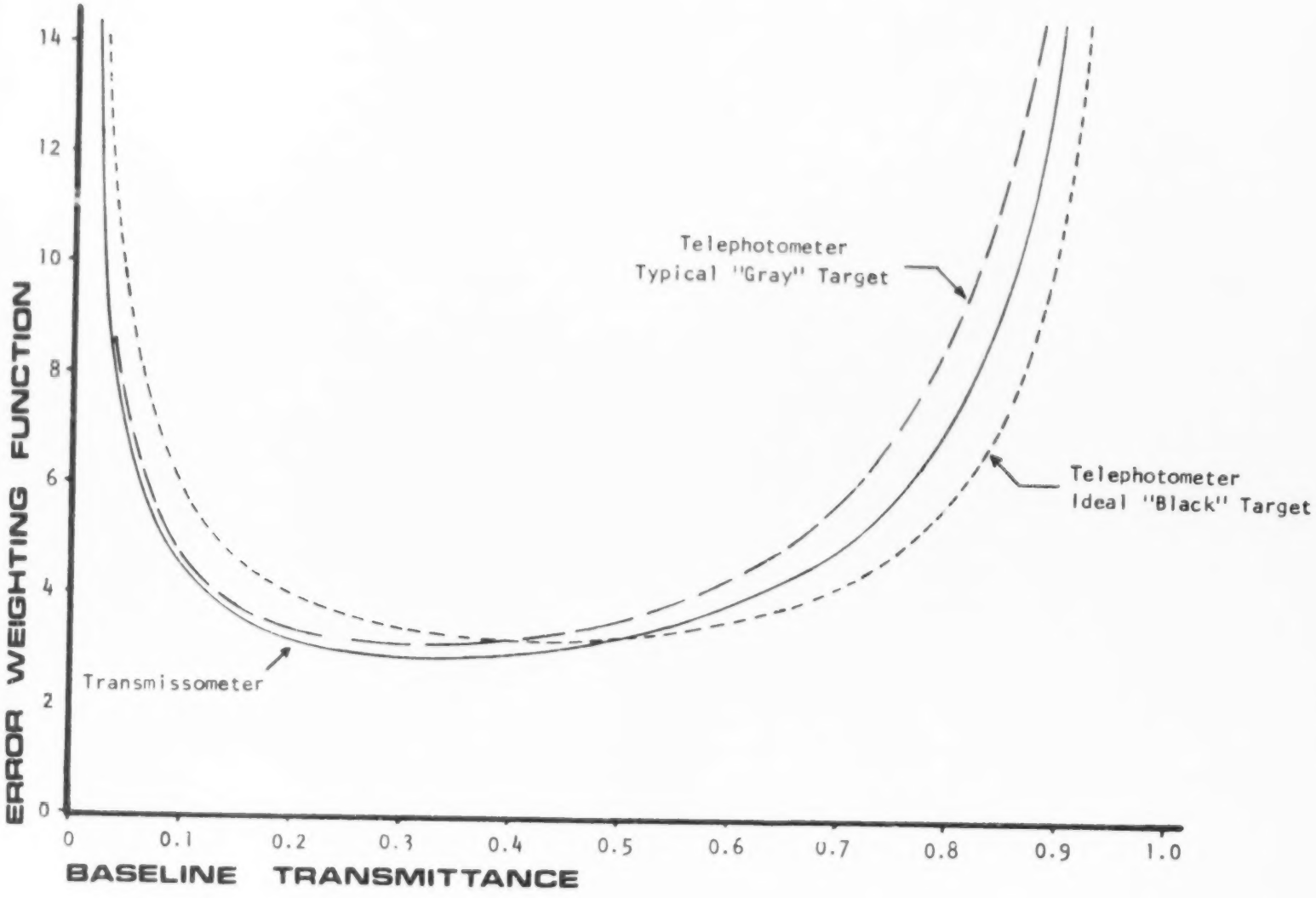

Figure A-2: Constant absolute measurement errors.

$$\epsilon^2_{B_{\infty}} = \epsilon^2_{B_h} + \frac{1}{(1-|C_o|)^2}\left[0.0001\,\epsilon^2_{R'} + 0.0121\,\epsilon^2_R\right] \quad \text{(A33)}$$

Substituting equation (A33) into equation (A27),

$$\epsilon_\tau = \frac{1}{|C_o|}\left\{\frac{(1-|C_o|\tau)^2}{\tau^2}\epsilon^2_{B_R} + \frac{(1-\tau)^2}{\tau^2}\epsilon^2_{B_h} + (1-|C_o|)^2\epsilon^2_{B_h} + 0.0001\,\epsilon^2_{R'} + 0.0121\,\epsilon^2_R\right\}^{1/2} \quad \text{(A34)}$$

The above equation may be rewritten in the form,

$$\epsilon_\tau = \frac{1}{|C_o|}\left\{\frac{(1-\tau)^2}{\tau^2}\epsilon^2_{B_R} + \frac{(1-\tau)^2}{\tau^2}\epsilon^2_{B_h} + \left[\frac{2(1-|C_o|)}{\tau} - (1-|C_o|^2)\right]\epsilon^2_{B_R} + (1-C_o)^2\epsilon^2_{B_h} + 0.0001\,\epsilon^2_{R'} + 0.0121\,\epsilon^2_R\right\}^{1/2} \quad \text{(A35)}$$

Again for the case, $\epsilon_{B_R} = \epsilon_{B_h} = \epsilon_B$,

$$\epsilon_\tau = \frac{1}{|C_o|}\left\{2\left[\frac{(1-\tau)^2}{\tau^2}\right]\epsilon^2_B + 2(1-|C_o|)\left[\frac{(1-|C_o|\tau)}{\tau}\right]\epsilon^2_B + 0.0001\,\epsilon^2_{R'} + 0.0121\,\epsilon^2_R\right\}^{1/2} \quad \text{(A36)}$$

Note now, that the first term in the braces constitutes the mean square transmittance error discussed earlier in relation to an ideal black target [equation (A28)]. For $B_\infty = 0$ (and therefore $R = 0$) equation (A36) in fact reduces to equation (A28). Assuming once more without loss of generality,

$$\epsilon^2_{R'} = \epsilon^2_R = \epsilon^2_\infty, \quad \text{(A37)}$$

equation (A36) may be rewritten,

$$\varepsilon_\tau = \frac{1}{|C_o|}\left\{2\left[\frac{(1-\tau)^2}{\tau^2}\right]\varepsilon_B^2 + 2(1-|C_o|)\left[\frac{(1-|C_o|\tau)}{\tau}\right]\varepsilon_B^2 + 0.0122\,\varepsilon_\rho^2\right\}^{1/2} \quad \text{(A38)}$$

Equation (A38) thus provides the basis for determining the further deleterious effect of viewing non-black targets for the estimate of visibility. To gain an idea of the magnitude of the effect in relation to viewing the ideal black objects, suppose mean square errors in the specification of target and foreground reflectances 100 times the mean square errors in the brightness measurements, i.e., $\varepsilon_\rho^2 = 100\,\varepsilon_B^2$. Equation (A38) may then be written,

$$\varepsilon_\tau = \frac{1}{|C_o|}\left\{2\left[\frac{(1-\tau)^2}{\tau^2}\right] + 2(1-|C_o|)\left[\frac{(1-|C_o|\tau)}{\tau}\right] + 1.22\right\}^{1/2}\varepsilon_B \quad \text{(A39)}$$

and therefore,

$$\varepsilon_V = \frac{\sqrt{2}}{|C_o|\ln\tau}\left\{\left[\frac{(1-\tau)^2}{\tau^2}\right] + (1-|C_o|)\left[\frac{(1-|C_o|\tau)}{\tau}\right] + 0.61\right\}^{1/2}\varepsilon_B \quad \text{(A40)}$$

With the values $R = R' = 0.1$ previously assumed,

$$\varepsilon_V = \frac{1.49}{\ln\tau}\left\{\left[\frac{(1-\tau)^2}{\tau^2}\right] + 0.05\left[\frac{1}{\tau} - 0.95\right] + 0.61\right\}^{1/2}\varepsilon_B \quad \text{(A41)}$$

Shown plotted in Figure 13, p. 48, as functions of τ, are the error weighting functions defined by the measurements error coefficient terms of equations (A30) and (A41). The impact of the reflectance specification errors in relation to gray-target telephotometric measurements is dramatic for the high baseline transmittances. In fact, the behavior of the telephotometer error weighting factor approaches that of the transmissometer, and this result is not unexpected. That is, consider [from equation (A23)] that for a gray target,

$$B_R = B_{go}\,\tau + B_h\,(1 - \tau). \quad \text{(A42)}$$

The first term on the right side of equation (A42) is the contribution to B_R from the intrinsic target brightness, a brightness which suffers attenuation over the telephotometer baseline according to the dictates of the Bouguer-Lambert law; the second term on the right side is the con-

tribution to B_R from light -- the so-called "air light" -- which is scattered to the telephotometer by the atmospheric aerosol along the telephotometer baseline. For the black object now, the ratio B_B/B_b -- the basic telephotometer datum -- provides the measure of the *compliment* of transmittance. For the gray object, and as $\tau \to 1.0$, however, the contribution of the air light to the total perceived target is relatively slight, and the ratio B_R/B_h becomes proportional to the transmittance, *per se*. That is, for a weak air-light contribution to B_R, the brightness ratio measurement becomes in effect a transmittance measurement, and the impact of a measurement error on the specification of the visibility therefore matches that of the transmissometer.

Differentiating equation (A41) with respect to τ, setting the result equal to zero and rearranging terms,

$$\ln \tau = - \frac{[1.385\ \tau^2 - 1.95\ \tau + 1]}{[1 - 0.975\ \tau]} \tag{A43}$$

The root of the above equation indicates a minimum visibility error in the typical gray target telephotometer measurements for a baseline telephotometer measurements for a baseline transmittance of about 0.49.

CONSTANT ABSOLUTE BRIGHTNESS ERRORS

IDEAL BLACK TARGET

For the case $B_o = 0, |C_o| = 1$, equation (A27) may be written,

$$\epsilon_\tau = \frac{(1-\tau)}{\tau} \left[\frac{\delta^2_{B_R}}{B^2_R} \quad \frac{\delta^2_{B_h}}{B^2_h} \right]^{1/2} \tag{A44}$$

From equation (A23) with $B_o = 0$,

$$B_R = B_h\ (1 - \tau); \tag{A45}$$

Therefore, again with $\delta_{B_R} = \delta_{B_h} = \delta_B$,

$$\epsilon_v = \frac{\delta_B}{B_h} \cdot \frac{\sqrt{2}}{\tau \ln \tau} \left[2 - 2\tau + \tau^2 \right]^{1/2} \tag{A46}$$

The error weighting factor of equation (A46) is shown plotted in Figure 13. The behavior of the factor is similar to that derived for the transmissometer for the case of constant absolute measurement errors. That is, a

rather broad functional minimum about the value, in this case, of τ = 0.43 degrades at both high and low baseline transmittances. For high transmittances, the telephotometer gives somewhat better results, whereas for low transmittances the transmissometer is the better instrument for visibility estimates.

Again for the illustrative case of a percent measurement errors and a desired 10 percent accuracy in the visibility estimate, Figure 13 indicates a $W_{tel}(\tau) \leq 5$ for transmittances in the range $0.13 \leq \tau \leq 0.76$. Over a one mile instrument baseline, visibility could be specified to the desired 10 percent accuracy in the range of about $1.4 \leq V \leq 10.5$ miles.

The equivalence of transmissometer and telephotometer measurement accuracies again occurs for a baseline transmittance τ = 0.5. This is to be expected; because whereas the transmissometer provides a direct measure of the transmittance [equation (A6)], the brightness values yielded by the telephotometer against an ideal black target provide, as mentioned earlier, the measure of the compliment of the transmittance. Given system measurement errors equal in magnitude (either relatively or absolutely), it is only when τ = 0.5 that the associated errors in the transmittance and its compliment are equal.

"GRAY" TARGET

For the parameter values stated earlier, the rms visibility error developed from equation (A35) for constant absolute measurement errors may be stated,

$$\epsilon_V = \frac{\epsilon_B}{B_h} \cdot \frac{1.05}{\ln \tau} \left(\frac{1}{\tau^2} + \frac{0.10}{(1-\tau)^2} \left[\frac{1}{\tau} - 0.975 \right] + 1.2225 \right)^{1/2} \qquad \text{(A47)}$$

In the above statement the value taken for $\epsilon_\rho^2 = 100\ (\epsilon_B/B_h)^2$.

The error weighting factor in equation (A47) is also shown plotted in Figure 13. The behavior of the factor is similar to that for the case of the ideal black target, and again shows the degradation of the visibility estimate as non-black targets are viewed over baselines with progressively greater transmittances. Differentiating equation (A47) with respect to τ, setting equal to zero, and rearranging terms,

$$\ln \tau = - \frac{[2.445(1-\tau)^3(0.82+\tau^2)+0.0195\tau(1-\tau)(10.26-\tau)]}{[2(1-\tau)^3+0.10(1-\tau)-0.0195\tau^2(10.26+\tau)]} \qquad \text{(A48)}$$

The root of the above equation indicates the minimum error at a baseline transmittance of about τ = 0.326.

NEPHELOMETER

The volume scattering coefficient is defined by,

$$b = 2\pi \int_0^{\pi} \beta(\theta) \sin\theta d\theta \qquad (A49)$$

where $\beta(\theta)$ is the so-called scattering phase function, i.e., the scattering cross section per unit volume of air per unit solid angle for beams scattered through an angle θ (Kerker, 1969). The function thus defines the directional characteristics of the energy scattered from a given scatterer, and the volume scattering coefficient is thus determined by collecting all the energy so scattered through all directions. The volume scattering is thus related to the power per unit solid angle per unit area of a detecting surface, B, by,

$$b = \frac{2\pi r_s^2}{I} B \qquad (A50)$$

where r_s is the radius of a spherical surface centered on the scattering particle (Middleton, 1943). Equation (A50) is the basic "calibration" equation of the Beutell and Brewer (1949) type nephelometer used during the field test program.

Ensor and Waggoner (1970) have discussed a fundamental error in instrumental techniques for measuring b according to equation (A49). They point out that in practice is it impossible to perform instrumentally the required integration over the full surface of a sphere. Rather, instrumental constraints result, in effect, in a "truncated" integration, viz.,

$$b' = 2\pi \int_{\theta_1}^{\pi/2} \beta(\theta) \sin\theta d\theta \qquad (A51)$$

with the result that b', the instrumentally derived volume scattering coefficient, is always less than the true value defined by equation (A49).

Rabinoff and Herman (1972) examined in greater detail the results of Ensor and Waggoner, and have in fact, suggested revised integrating nephelometer calibration equations for minimizing the angular truncation error. They present the magnitude of the error as the ratio of b'/b, and as a function of size of the scattering particles. The parameter used to characterize particle size is the exponent, ν, of the Junge size law distribution,

$$\frac{dN}{d(\log r)} = Cr^{-2} , \qquad (A52)$$

where N is the particle number density in the size interval d(log r) The relative error in the volume scattering coefficient as defined by equation (A7) in terms of the ratio b'/b, is,

$$\frac{\Delta b}{b} = 1 - \frac{b'}{b} \qquad (A53)$$

Based on Rabinoff and Herman's data, the plot of the relative error in the volume scattering coefficient as a function of the Junge distribution size parameter is as shown in Figure A-1.

Note that the error is larger the smaller the size parameter. A small size parameter implies a relatively large number of large-size particles in the size distribution [equation (A52)]. The larger the particle, the more asymmetric the scattering phase function becomes, departing more and more from the complete symmetry of the Rayleigh scattering function. That is, very large particles are characterized by a strong scattering lobe in the forward direction. The angular truncation error that is the basis of Figure 14 would thus be more severe in this case, effectively "neglecting" a greater proportion of the scattered radiation in the radiation measurement.

Although Figure 14 does not present the picture of the relative error in the nephelometer measurement as a function of transmittance or visibility [illegible] as was done previously (to do so would require [illegible] knowledge of the size distribution as a function of visibility), qualitatively it may be stated that the nephelometer is likely to afford the better measurement results the clearer the air. That is, good visibility implies not only a relatively low particle loading [illegible], but also smaller particles (ergo, larger values of $\langle v \rangle$) in that loading. The limit here is the perfectly clear atmosphere at the limit of Rayleigh scattering by air molecules. Industrial pollution likely results in poor visibility due to relatively large scattering particles.

ERROR SOURCES

In the development of the error analysis, no specific mention of the [illegible] of error in the measurements performed by the different instrument systems has been made, other than for the case of the nephelometer. Such specification becomes especially important for the transmissometer and telephotometer measurements because of the effect of error [illegible] (i.e., constant relative or constant absolute) on the final visibility estimate. This effect is therefore amplified in the following discussion.

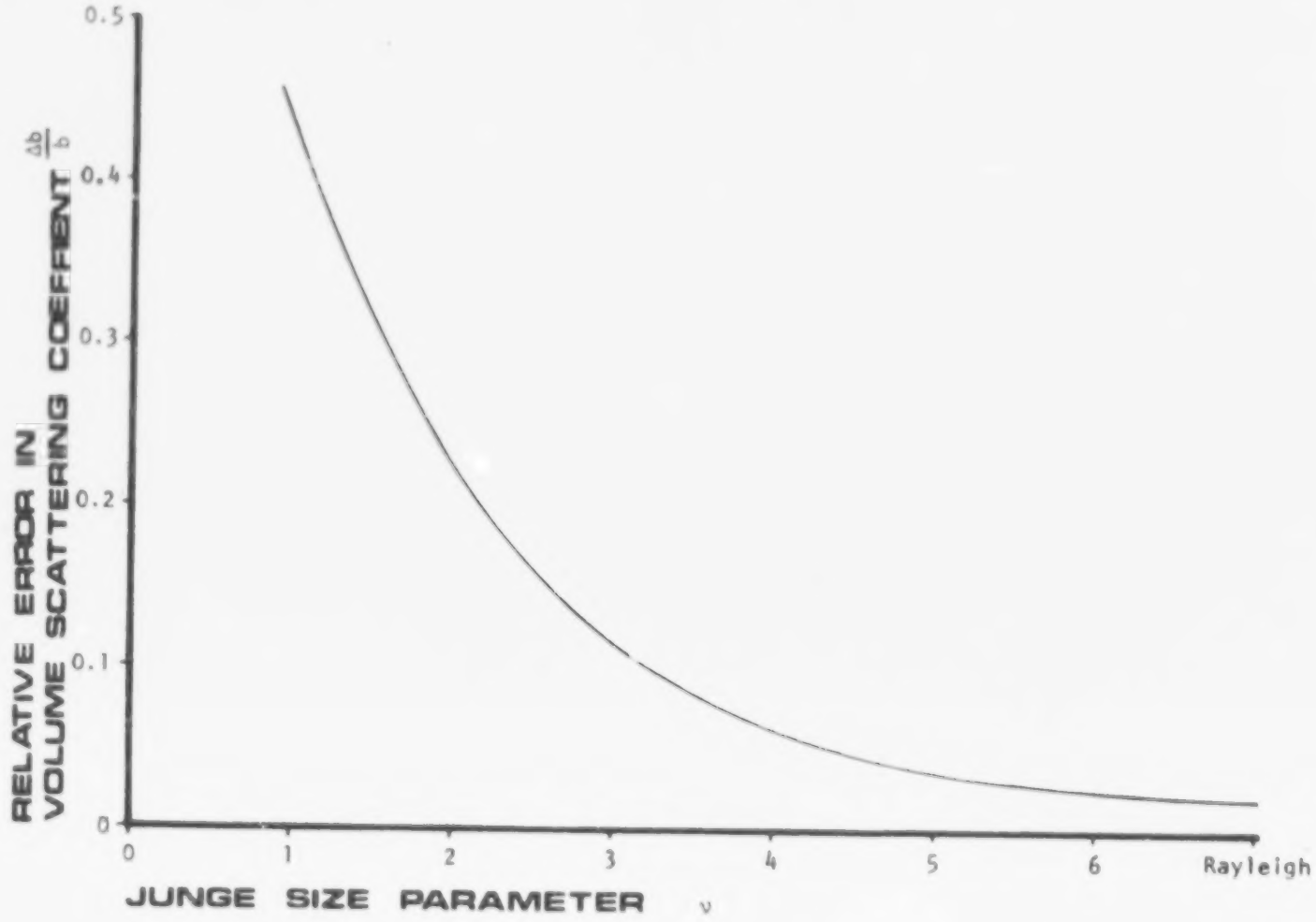

Figure A-3: Relative error in the volume scattering coefficient.

TRANSMISSOMETER

A light beam propagated through the atmosphere is subject not only to attenuation by particles of the atmospheric aerosol, but also to a variety of refractive effects including beam bending, scintillation, jitter, and beam broadening (see, for example, *Beckmann, 1965*). Beam bending is in response to the overall gradient in optical refractive index, whereas the other phenomena are in response to turbulence in the refractive index field. Scintillation and jitter are stocastic processes, and manifest themselves in received signals as random fluctuations about the average received signal level. A simple time-averaging process is therefore sufficient to remove their effects on the measurement of that average signal level.

However, beam bending by gross refraction and beam spreading due to turbulence is likely to result in systematic errors by causing loss of a fraction of the beam to the detector's field-of-view. How much would be lost at any time would depend on the atmospheric structure while the measurement was being performed. However, for a given atmospheric structure, the actual magnitude of the error increment ΔI, would depend on the average signal level. That is, beam bending and spreading losses can be considered measurement errors of the constant relative error type.

Electronic noise would constitute the example of a constant absolute measurement error. That is, if the electronic noise could be isolated from the overall measurement error, it would be found to be independent of the average signal level. Suppose then, the received signal error increment is written as the sum of the electronic and refractive "noise," ΔI_e and ΔI_r, respectively; i.e.,

$$\Delta I = \Delta I_e + \Delta I_r \tag{A54}$$

The relative error would thus be,

$$\frac{\Delta I}{I} = \frac{\Delta I_e}{I} + \frac{\Delta I_r}{I} \tag{A55}$$

For large I (good visibility) the second term on the right side of equation (A55)is likely to dominate, whereas for small I (poor visibility) (assuming $\Delta I_r/I$ - constant as just argued) the first term would dominate. The net result is that the true error weighting factor for the transmissometer should be a composite of Figures A-1 and A-2. That is, for low baseline transmittances implying poor visibility, the factor to be used is represented by the left side of Figure A-1, whereas for high baseline transmittances (good visibility) the factor is according to the right side of Figure13. This composite is as shown in Figure A-4.

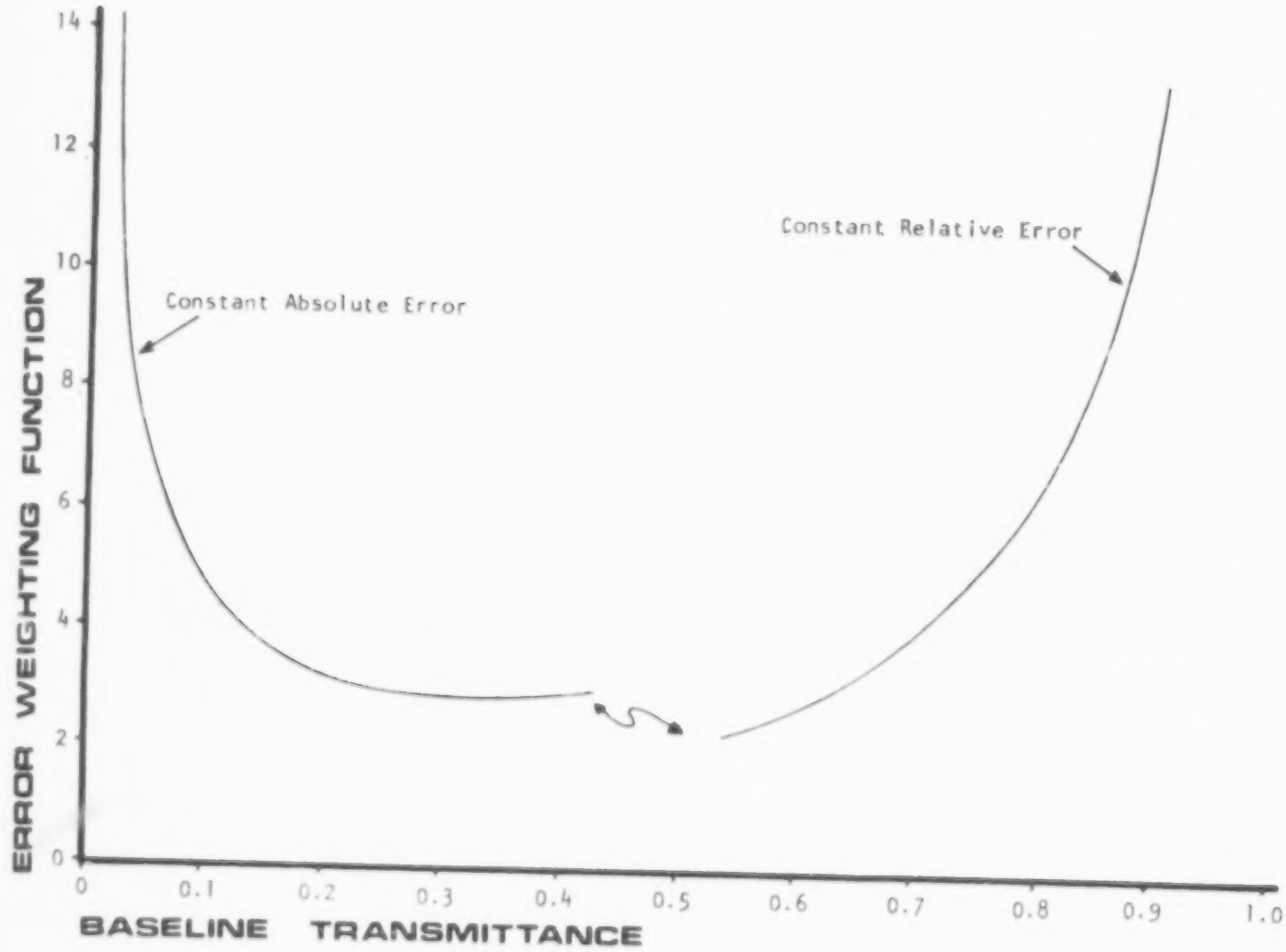

Figure A-4: Composite error weighting function - Transmissometer.

TELEPHOTOMETER

The error most often cited in regard to telephotometer measurements is that due to "scattered in" light, i.e., light scattered to the instrument detector from the interior surfaces of the instrument collecting optics (Middleton, 1952). Again the argument can be made that such an error would be of the constant relative error type, insofar as the incremental value of the scattered in light would be proportional to the average light level of surrounding environment, i.e., to the surrounding "air light". Again, the constant absolute error would be associated with electronic noise.

In normal daytime operation, telephotometer measurement errors will impact most strongly on the measurement of the apparent target brightness because of the inherently lower average signal levels for the target as compared to the horizon brightness. For high baseline transmittance values (good visibility, and therefore very dark targets) it is thus conceivable that electronic noise -- the constant absolute error -- could dominate in the target brightness measurement. Otherwise, it is the constant relative error which would also characterize the telephotometer measurements. Again, as argued previously, the composite error weighting function would have to be specified as shown in Figure A-5.

Regarding Figure 16 it is important to emphasize that with "natural" targets, the tendency is to intuitively select "targets" which are the most accurate instrument measurements. That is, targets will be selected that are neither so far that they are about at the liminal contrast (low baseline transmittances), nor so close that there is no appreciable "air light" contributing to the apparent target brightness (high baseline visibility). Referring to the conclusions then (Section I), a very distinct advantage of the telephotometer for visibility measurements can be stated, viz., the ability for selection of a variable baseline to assure the minimum measurement error (the minimum in the weighting function curve), and therefore the minimum error in the associated visibility estimate. Such selection is possible because of the remarkably small residual error in the visibility estimate, if only gross assumptions are used to correct contrast measurements for the effects of intrinsic brightness of "gray," as opposed to completely black targets.

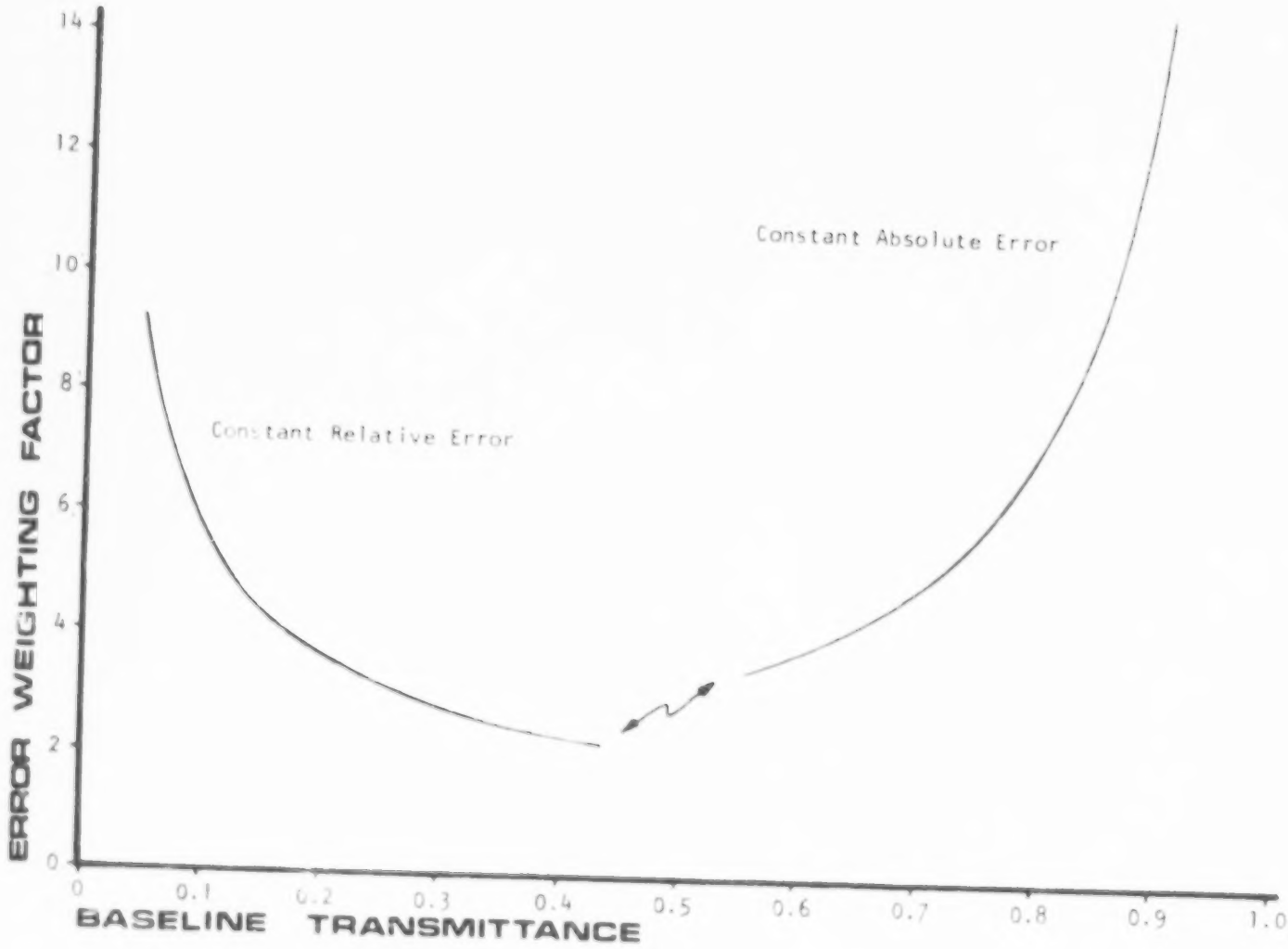

Figure A-5: Composite error weighting function - Telephotometer.

APPENDIX B

Observations

Date (Mo./Day)	Time (Hour)	OBS (10^{3}m)	APVIS (10^{3}m)	NEPH (10^{-4} m^{-1})	$\overline{NEPH}$ (10^{-4} m^{-1})	TRANS (10^{-4} m^{-1})	TELE (10^{-4} m^{-1})	TEMP (°F)	RH (%)
8/9	0915	11.3	20.1	1.3		3.74	2.41	70	71
8/9	1215	11.3	14.5	2.0		5.18	4.41	74	55
8/9	1515	19.3	19.3	1.4		1.44	1.99	82	47
8/10	0710	16.1	4.8	1.8		1.15	2.45	58	83
8/10	1010	17.7	16.1	0.8		1.15	1.27	60	74
8/10	1310	16.1	16.1	1.1		2.88	1.63	65	58
8/14	0910	19.3	12.1	1.2	1.5	4.32	2.45	60	80
8/14	1200	16.1	12.9	2.0	1.9	5.76	2.21	66	65
8/14	1500	18.6	21.7	1.6	1.5	7.20	1.72	72	55
8/15	0910	4.0	2.4	2.9	2.5	11.23	5.03	54	94
8/15	1200	8.0	6.4	2.2	2.0	6.34	2.62	58	80
8/15	1500	8.9	6.4	2.6	2.5	6.62	2.92	62	70
8/16	1000	17.7	8.9	1.2	1.2	7.78	0.97	57	83
8/20	1000	24.1	32.2	1.0	1.0	8.06	1.20	60	64
8/23	1120	16.1	14.5	3.3	2.5	4.32	3.29	59	75
8/23	1420	18.6	12.1	2.6	2.0	5.76	1.51	60	69
8/25	0900	16.1	24.1	1.2	1.5	10.08	1.36	52	80
8/28	1200	16.1	24.1	0.9	1.2	3.17	1.37	66	56
8/28	1500	16.1	21.7	0.6	1.0	3.46	1.05	68	61
8/28	1800	16.1	20.1	1.3	1.0	0.29	1.18	68	63
8/29	1000	11.3	8.9	2.8	2.5	6.34	2.26	61	80
8/29	1300	14.5	16.1	1.8	1.2	3.46	2.38	66	65
8/29	1600	18.6	24.1	1.8	1.6	2.02	1.10	69	56
8/30	1000	17.7	17.7	1.0	1.3	4.03	1.10	58	71
8/30	1300	14.5	17.7	1.0	1.1	2.59	1.99	58	71
8/31	1300	24.1	17.7	1.1	1.1	1.15	1.60	57	72
9/1	1100	21.7	24.1	1.3	1.4	5.76	1.64	65	48
9/4	0930	24.1	44.3	1.2	1.3	5.76	1.94	62	70
9/5	1100	8.0	32.2	2.5	2.4	7.49	2.74	79	69
9/5	1400	19.3	24.1	1.1	1.5	3.46	1.57	87	33

APPENDIX B (cont'd)

Observations

Date (Mo./Day)	Time (Hour)	OBS (10^{5} m)	APVIS (10^{3} m)	NEPH (10^{-4} m^{-1})	$\overline{NEPH}$ (10^{-4} m^{-1})	TRANS (10^{-4} m^{-1})	TELE (10^{-4} m^{-1})	TEMP (°F)	RH (%)
9/6	1000	24.1	24.1	1.1	1.3	8.64	1.27	64	75
9/6	1300	17.7	17.7	0.6	1.2	2.88	1.76	65	72
9/6	1600	16.1	9.7	0.5	1.0	8.64	1.36	64	93
9/7	0900	15.3	18.5	1.0	1.2	7.20	1.89	57	90
9/7	1200	22.5	24.1	1.0	1.2	6.34	1.57	62	72
9/7	1500	22.5	22.2	1.0	1.0	2.88	1.52	67	58
9/8	0800	8.9	9.7	1.0	1.0	11.52	2.26	50	100
9/8	1100	16.1	12.9	1.8	1.7	7.49	1.89	64	60
9/10	0900	72.9	72.4	1.0	1.4	7.49	1.56	67	75
9/10	1200	62.6	64.3	1.0	1.0	4.32	1.60	74	57
9/10	1500	80.9	80.5	1.0	1.0	6.05	1.68	82	47
9/11	0900	8.9	5.6	1.5	1.5	6.62	3.23	58	93
9/11	1200	11.3	11.3	1.6	1.6	6.62	2.70	64	75
9/11	1500	20.9	20.1	1.1	1.3	3.46	1.74	70	61
9/11	1800	20.9	24.1	1.3	1.2	1.73	1.65	70	63
9/12	1030	12.9	3.2	2.0	2.0	10.08	3.23	57	89
9/12	1330	12.9	8.9	2.1	1.9	6.05	2.35	61	83
9/12	1630	15.3	9.7	2.0	2.0	2.02	2.38	68	58
9/13	1200	8.9	5.6	2.8	2.0	4.61	3.62	61	83
9/13	1500	12.1	20.1	2.0	2.2	0.29	1.99	70	58
9/13	1800	19.3	24.1	1.0	1.2	0.29	1.41	71	45
9/14	0900	14.5	20.1	2.0	2.0	7.49	2.26	60	74
9/14	1200	14.5	20.1	1.8	1.5	7.20	2.32	60	78
9/14	1500	15.3	20.1	1.6	1.5	4.90	1.87	68	52
9/14	1800	17.7	20.1	1.6	1.6	2.30	1.78	69	48
9/15	0900	16.1	13.7	2.0	2.7	10.37	1.89	59	69
9/15	1200	24.1	20.1	1.2	1.5	7.49	1.43	74	31
9/15	1500	24.1	24.1	1.3	1.4	7.20	1.59	77	28
9/16	1000	32.2	44.3	2.1	2.0	9.22	1.81	64	41
9/16	1300	28.2	44.3	0.9	0.9	4.61	1.36	79	24
9/17	0900	16.1	20.1	2.0	1.6	8.64	1.72	57	64
9/17	1200	16.9	24.1	1.7	1.5	4.32	1.93	68	50
9/17	1500	19.3	24.1	1.6	1.5	1.73	1.90	68	50
9/17	1800	19.3	20.1	1.0	1.1	2.88	1.62	66	62
9/18	0900	22.5	21.7	0.9	0.9	7.49	1.71	60	93
9/18	1200	23.3	24.1	1.2	0.9	4.32	1.71	62	80
9/18	1500	23.3	24.1	1.1	0.9	4.32	1.50	63	72

APPENDIX B (cont.)

Observations

Date (Mo./Day)	Time (Hour)	OBS (10^{3}m)	APVIS (10^{3}m)	NEPH (10^{-4}m^{-1})	$\overline{\text{NEPH}}$ (10^{-4}m^{-1})	TRANS (10^{-4}m^{-1})	TELE (10^{-4}m^{-1})	TEMP (°F)	RH (%)
9/18	1800	28.2	24.1	0.9	0.8	0.86	1.18	64	60
9/19	0900	8.0	13.7	1.3	1.0	5.18	3.29	55	96
9/19	1200	7.2	7.2	1.1	1.0	7.20	3.18	59	89
9/19	1500	8.0	4.8	1.1	1.0	10.08	3.12	60	100
9/19	1800	20.1	11.3	0.9	0.8	5.76	1.65	61	95
9/20	0900	24.1	19.6	0.7	0.7	15.84	1.03	59	89
9/20	1200	21.7	15.3	0.5	0.5	12.96	1.22	59	89
9/20	1500	6.9	12.1	0.5	0.5	21.60	5.03	60	100
9/20	1800	22.5	18.5	0.5	0.5	8.64	0.65	60	93
9/21	0900	32.5	24.1	0.8	0.8	10.08	1.62	58	95
9/21	1200	22.5	20.1	0.5	0.6	8.64	1.18	61	93
9/21	1500	19.6	17.7	1.3	1.0	0.58	1.85	61	93
9/21	1800	28.2	28.2	0.6	1.0	1.44	0.84	62	86
9/24	1200	11.3	8.0	0.8		8.35	1.59	59	89
9/24	1500	16.1	15.3	1.1		2.30	1.81	60	86
9/25	0900	19.3	17.7	0.9	1.0	4.32	1.29	56	83
9/25	1200	25.7	20.1	0.5	0.7	6.91	1.02	59	66
9/25	1500	25.7	48.3	0.3	0.6	5.76	1.04	66	44
9/25	1800	26.6	44.3	0.5	0.7	0.29	1.27	66	44
9/26	0900	24.1	32.2	1.4	1.1	2.30	1.19	58	69
9/26	1200	28.2	68.4	0.5	0.8	2.30	1.06	69	46
9/26	1500	24.1	72.4	1.0	1.0	1.44	1.34	72	49
9/27	1200	8.9	8.0	2.8	2.8	8.64	4.02	66	75
9/27	1500	16.1	24.1	1.9	1.8	3.17	2.32	76	51
9/27	1800	24.1	32.2	1.0	1.2	0.29	1.12	73	54
9/28	0900	0.3	0.8	2.5	2.7	28.80	45.20	53	96
9/28	1200	7.2	6.1	4.8	4.8	15.84	7.87	64	80
9/28	1500	12.1	24.1	2.5	3.1	1.73	2.83	74	59
9/28	1800	22.5	32.2	1.9	2.3	0.29	1.51	75	57
9/29	0900	3.2	8.0	3.5	4.9	7.20	11.30	59	88
9/29	1200	16.9	14.5	0.9	1.5	0.29	1.10	62	77
9/30	1300	24.1	32.2	1.2	1.1	3.74	0.76	62	45
9/30	1600	48.3	32.2	0.9	1.0	1.15	1.12	66	52

APPENDIX B (cont.)

Observations

Date (Mo./Day)	Time (Hour)	OBS (10^3m)	APVIS (10^3m)	NEPH (10^{-4} m^{-1})	$\overline{NEPH}$ (10^{-4} m^{-1})	TRANS (10^{-4} m^{-1})	TELE (10^{-4} m^{-1})	TEMP (°F)	RH (%)
10/1	1000	16.1	17.7	1.3	1.4	3.46	1.81	52	82
10/1	1300	32.2	17.7	1.0	1.3	1.44	1.31	55	74
10/1	1600	32.2	32.2	1.1	1.2	1.44	1.21	59	61
10/2	0900	12.9	10.5	2.2	2.1	6.91	2.38	48	92
10/2	1200	22.5	16.1	1.5	1.5	5.18	1.74	57	69
10/2	1500	24.1	20.1	1.2	1.3	1.73	1.53	60	55
10/2	1800	24.1	24.1	1.3	1.3	0.58	1.17	60	53
10/3	0900	13.7	4.0	2.0	2.0	6.34	1.38	43	92
10/3	1200	10.5	7.2	2.5	2.4	8.01	3.48	58	66
10/3	1500	18.5	13.7	1.6	1.9	5.47	1.85	62	51
10/3	1800	2.5	17.7	1.2	1.5	0.29	1.59	61	51
10/4	0900	5.6	5.6	2.8	2.8	28.80	3.94	42	93
10/4	1200	14.5	11.3	2.3	2.8	7.20	2.32	56	59
10/4	1500	17.7	21.7	2.0	2.0	4.61	2.01	61	57
10/4	1800	22.5	24.1	1.1	1.4	0.29	1.10	58	55
10/5	0900	11.2	11.3	2.0	1.8	4.03	2.78	52	92
10/5	1200	17.7	12.1	2.2	2.0	4.89	2.70	54	89
10/8	0900	48.3	52.3	1.1	1.2	7.20	1.72	52	74
10/8	1200	36.2	52.3	1.0	1.0	4.61	1.50	59	51
10/8	1500	36.2	4.1	1.0	0.9	0.59	1.19	64	52
10/8	1800	25.7	40.3	1.4	1.3	0.29	1.47	64	64
10/9	1200	16.1	13.7	1.8	1.8	3.46	2.10	54	74
10/9	1500	17.7	24.1	1.8	1.7	1.44	2.10	60	61
10/9	1800	20.9	29.0	1.2	1.3	0.29	1.15	58	59
10/10	0900	12.1	12.1	2.0	1.9	6.34	2.53	49	89
10/1	1200	9.7	16.1	1.3	1.4	4.32	1.02	54	77
10/1	1500	4.8	7.2	1.0	1.0	4.32	4.11	56	83
10/11	1000	9.5	8.9	1.5	1.6	6.91	3.23	52	96
10/15	0900	4.2	8.5	2.2	2.0	11.52	5.84	46	96
10/15	1200	4.8	4.8	2.9		9.79	6.03	55	83
10/15	1500	10.5	6.4	3.0	3.1	4.61	3.55	57	80
10/15	1800	9.7	8.0	2.5	2.7	9.64	5.32	55	92
10/16	0900	8.9	12.9	2.0	1.9	23.04	4.13	54	96
10/16	1200	18.5	18.5	1.2	1.3	8.06	0.98	60	74
10/16	1500	18.5	26.5	1.5	1.7	3.17	2.13	63	69

APPENDIX B (cont.)

Observations

Date (Mo./Day)	Time (Hour)	OBS (10^{3} m)	APVIS (10^{3} m)	NEPH (10^{-4} m^{-1})	$\overline{NEPH}$ (10^{-4} m^{-1})	TRANS (10^{-4} m^{-1})	TELE (10^{-4} m^{-1})	TEMP (°F)	RH (%)
10/16	1800	21.7	18.5	1.2	1.5	0.29	1.08	58	74
10/17	0900	4.0	2.4	3.0	2.1	28.80	15.08	44	96
10/17	1200	12.9	10.5	2.1	2.0	8.93	2.59	62	74
10/17	1500	15.3	18.5	2.0	2.0	2.88	2.29	70	56
10/17	1800	20.9	56.3	1.3	2.5	0.29	1.08	64	69
10/18	0900	26.6	23.3	1.8	1.7	23.04	2.51	51	92
10/18	1200	24.9	26.6	1.4	1.3	4.61	1.43	66	67
10/18	1500	19.3	52.3	1.9	1.9	0.86	1.91	68	60
10/19	0900	1.6	7.2	3.0	2.2	27.36	12.07	51	100
10/19	1200	14.5	8.0	2.6	2.6	7.20	2.62	58	83
10/19	1500	13.7	13.7	2.0	2.0	4.32	2.15	60	74
10/19	1800	11.3	11.3	3.3	3.0	2.88	2.59	57	77
10/22	0900	6.4	26.6	2.5	2.3	5.32	48	94	
10/22	1200	28.2	22.5	2.0	2.3	5.76	1.71	55	94
10/22	1500	13.7	22.5	2.1	2.0	7.20	1.99	58	80

* Time averages could not be obtained for these data
** One-hour average centered on the identified time

APPENDIX C

24 HOUR SUSPENDED PARTICULATE CONCENTRATIONS

(gm^{-3})

Date	Central Site	PSAPCA Site
8/1	--	53
8/7	--	44
8/11	32	--
8/12	39	--
8/13	19	25
8/14	20	--
8/15	36	--
8/16	7	--
8/17	10	--
8/18	12	--
8/19	16	28
8/20	18	--
8/21	17	--
8/22	19	--
8/23	22	--
8/25	--	48
8/31	--	52
9/6	--	26
9/12	--	50
9/18	--	26
9/24	--	30
9/30	--	24
10/6	--	25
10/9	48	--
10/10	37	--
10/12	--	22
10/15	45	--
10/16	41	--
10/17	40	--
10/18	40	38
10/19	55	--
10/24	--	23
10/30	--	26

APPENDIX D

SCATTERING COEFFICIENTS

$(10^{-4} m^{-1})$

Remote Nephelometer	Remote Neph. Central Site	Stationary Nephelometer	Date	Time	Remote Site Range from Central Site
	2.0	1.8	8-29	1300	
	0.8	1.0	9-6	1300	
	0.9	1.1	9-6	1600	
0.8	0.9	1.0	9-10	1200	1.8 km SSW
0.9	0.9	1.0	9-10	1500	1.4 km E
1.2	1.1	1.1	9-11	1500	1.5 km NE
1.3	1.3	1.3	9-11	1800	1.8 km SSW
1.8	2.5	2.1	9-12	1330	1.4 km E
2.1	1.9	2.0	9-12	1630	5.3 km N
	3.1	2.8	9-13	1200	
2.0	1.95	1.95	9-13	1500	1.8 km SSW
0.95	1.0	1.0	9-13	1800	1.0 km E
	2.2	2.0	9-14	0900	
1.85	1.8	1.8	9-14	1200	2.5 km NE
1.65	1.6	1.6	9-14	1500	1.0 km N
1.5	1.6	1.6	9-14	1800	1.8 km SSW
3.0	2.0	2.0	9-15	0900	2.5 km SSE
1.5	1.1	1.2	9-15	1200	5.8 km SSE
1.1	1.05	1.3	9-15	1500	1.8 km SSW
2.2	2.1	2.1	9-16	1000	1.0 km NNW
	1.0	0.9	9-16	1300	
2.05	2.0	2.0	9-17	0900	1.8 km SSW
1.6	1.9	1.7	9-17	1200	8.0 km SSE
1.4	1.4	1.6	9-17	1500	1.4 km E
1.4		0.9	9-18	0900	3.2 km ESE
	1.0	1.2	9-18	1200	
0.9		1.1	9-18	1500	3.4 km N
0.9	0.8	0.85	9-18	1800	1.8 km SSW
1.0	1.1	0.9	9-25	0900	3.2 km ESE
	0.5	0.5	9-25	1200	
	0.4	0.3	9-25	1500	
2.1	1.7	1.9	9-27	1500	13.6 km SSE
3.8	4.9	4.8	9-28	1200	3.4 km N
2.1	2.1	2.5	9-28	1500	5.6 km S

Remote Nephelometer	Remote Neph. Central Site	Stationary Nephelometer	Date	Time	Remote Site Range from Central Site
1.8	1.5	1.9	9-28	1800	4.4 km NNE
0.95	0.8	0.9	9-29	1200	4.4 km NNE
1.4	1.4	1.25	10-1	1000	1.8 km SSW
1.0	1.0	1.01	10-1	1300	3.2 km SE
0.9	0.8	1.05	10-1	1600	1.4 km E
1.2	1.1	1.5	10-2	1200	1.5 km N
0.9		1.2	10-2	1500	4.8 km SE
	2.2	2.0	10-3	0900	
2.5	2.6	2.5	10-3	1200	4.8 km SE
1.6	1.1	1.6	10-3	1500	12.8 km S
	1.1	1.2	10-3	1800	
1.5	1.8	2.3	10-4	1200	1.6 km N
1.7	1.5	2.0	10-4	1500	3.4 km N
	1.0	1.1	10-4	1800	
1.2	1.3	1.6	10-8	1800	32.0 km NNW
2.5	1.8	1.8	10-9	1200	4.0 km NNE
1.7		1.8	10-9	1500	1.6 km N
3.8	3.8	4.0	10-15	1200	1.4 km E
	4.0	3.0	10-15	1500	

REFERENCES

A1. Middleton, W. E. K., *Vision Through the Atmosphere*. University of Toronto Press. 1952. 250 pp.

A2. Stewart, H. S. and R. F. Hopfield. "Atmospheric Effects," *Applied Optics and Optical Engineering*. R. Ringslake, Editor, Academic Press, New York. 1965.

A3. List, Robert J. "Smithsonian Meteorological Tables." Smithsonian Institution, Washington, D.C. 1951. 527 pp.

A4. Kerker, M. *The Scattering of Light and Other Electromagnetic Radiation*. Academic Press, New York. 1969.

A5. Beutell, R. G., and A. W. Brewer. "Instruments for the Measurement of Visible Range." *J. Sci. Instr.* 26: 357-359. 1949.

A6. Ensor, D. S. and A. P. Waggoner. "Angular Truncation Error in the Integrating Nephelometer." *Atmos. Environ.* 4: 481-487. 1970.

A7. Rabinoff, R. A. and B. M. Herman. "Effect of Aersol Size Distribution on the Accuracy of the Integrating Nephelometer." *J. Appl. Meteor.* 12, 184-186. 1973.

A8. Beckmann, P. "Signal Degeneration in Laser Beams Propagated Through a Turbulent Atmosphere." *Radio Science*. 6y0: 629-640. 1965.